Arch Appl Mech (2011) 81: 451–472
DOI 10.1007/s00419-010-0421-z

ORIGINAL

Chun Nam Wong · Hong-Zhong Huang · Jingqi Xiong · Hua Long Lan

Generalized-order perturbation with explicit coefficient for damage detection of modular beam

Received: 20 May 2009 / Accepted: 25 February 2010 / Published online: 14 March 2010

Abstract A general method is formulated to estimate damage location and extent from the explicit perturbation terms in specific set of eigenvectors and eigenvalues. At first, perturbed orthonormal equation is generated from the perturbation of eigenvectors and eigenvalues to obtain the *k*-th explicit perturbation coefficients. At second, perturbed eigenvalue equation is generated from the perturbation of eigenvector and eigenvalue, and first-order expansion of the stiffness matrix to obtain other explicit perturbation coefficients. Stiffness parameters are computed from these equations using an optimization method. The algorithm is iterative and terminates under certain criteria. A fixed–fixed modular beam with various numbers of elements is used as test structure to investigate the applicability of the developed approach. By comparison with the Euler–Bernoulli beam, discretization errors are analyzed. In six elements beam, first-order algorithm converges faster for small percentage damage. Second-order algorithm is more efficient for medium percentage damage. For large percentage damage, the second-order algorithm converges more effectively. Meanwhile, for eight elements large percentage damage and ten elements small percentage damage, second-order algorithm converges faster to the termination criterion.

Keywords Explicit coefficient · Perturbed eigenvector · Perturbed eigenvalue · Modular beam · Damage detection

1 Introduction

Perturbation of eigenvalue had been reported in early literature [1]. Later, extensive perturbation analyses were ignited since the general mathematical skeleton of eigenvalue perturbation problem established by Wilkenson [2] and Bellman [3]. Power series was used by Romstad [4] to formulate general perturbation approach using holographic interferometry to determine the vibration modes of prototype experimentally. Stetson [5] predicted the perturbation effect of small changes in prototype parameter. In gyroscopic systems for small internal and external damping, Meirovitch and Ryland [6,7] used modal perturbation technique. Rayleigh's work was extended by Jones [8] on the general perturbation form of frequency and mode shape changes. Besides,

C. N. Wong (✉) · H.-Z. Huang · J. Xiong
School of Mechatronic, Mechanical, Electronic and Industrial Engineering,
University of Electronic Science and Technology of China, No.4 Section 2,
Jianshe North Road, 610054 Chengdu, Sichuan, People's Republic of China
E-mail: znhuang@uestc.edu.cn
Tel.: +86-028-83207035
Fax: +86-028-83206828

H. L. Lan
Jinchuan Group Ltd., Gansu, People's Republic of China

different researchers developed perturbation approaches to deal with systems consisted of distinct eigenvalues [9–11], repeated eigenvalue [12,13] and closely spaced modes [14].

In the area of structural design, Wanxie and Gengdong [15] made use of stationarity of Rayleigh quotient in second-order sensitivity analysis of multimodal eigenvalues. Then the method was applied to formulate a sequential quadratic programming approach in multimodal optimal design of structures. Wicher and Nalecy [16] determined the second-order sensitivity matrix and logarithmic sensitivity functions in the frequency domain. The second-order logarithmic sensitivity function was generated. Ryland and Meirovitch [17] established second-order perturbation approach for the response of perturbed, undamped and nongyroscopic dynamic systems where small changes in system mass and stiffness parameters initiated the eigenparameter perturbation. Second-order perturbation analysis of torsionally coupled building was carried out by Kan and Chopra [18,19]. The approach was applied to estimate the maximum response of a class of torsionally coupled, multistory buildings due to earthquake ground motion characterized by response spectra. Tsicnias and Hutchinson [20] made use of perturbation analysis in torsionally coupled buildings to obtain an approximation of the dynamic properties of the buildings in question by combining appropriately the dynamic properties of the corresponding buildings.

Innovative part of this work is to derive the generalized-order coefficients where they can be applied to common engineering systems. For the previous approach [9], perturbation coefficients were constructed from the basic vectors of all used eigenvectors and their coefficients. The technique developed here aims for evaluating generalized-order terms explicitly, so that the generalized-order perturbation coefficients can be constructed in sequential order. The advantage being that higher-order terms can be constructed efficiently and consecutively from the lower-order terms. This is essential when generalized-order terms become complicated. It is a methodology applicable to damage detection in different industries, such as aviation dynamic systems, electrical transmission facilities [21] and turbine components. Also, it can be applied to civilian structures, such as buildings and bridges.

2 Theoretical development

We derive here the derivatives of the eigenvalues and eigenvectors in the system equations from the eigenvalue problem. Consider here a self-adjoint system with distinct eigenvalues, its eigenvalue problem of the structure before the estimation is

$$K\overline{\phi}^k = \lambda^k M\overline{\phi}^k \tag{1}$$

where K, M are its system stiffness and mass matrices, and λ^k, $\overline{\phi}^k$ are its k-th eigenvalue and eigenvector. The eigenvalue problem of the damaged structure is

$$K_d\overline{\phi}_d^k = \lambda_d^k M\overline{\phi}_d^k \tag{2}$$

where K_d is its system stiffness matrix, and λ_d^k, $\overline{\phi}_d^k$ are its k-th eigenvalue and eigenvector. Using the first-order perturbation equation, the matrix K_d is related to K through

$$K_d = K + \sum_{d=1}^{m} \frac{\partial K}{\partial G_d}\delta G_d \tag{3}$$

where higher-order perturbations of K with respect to the damaged stiffness parameter G_d vanish by assuming K is a first-order function of G_d. m is the total number of stiffness parameters involved. The k-th eigenvalue and eigenvector of the damaged structure are related to λ^k and $\overline{\phi}^k$ through the generalized-order perturbation expansion equations:

$$\lambda_d^k = \lambda^k + \sum_{d=1}^{m}\lambda_{(1)d}^k\delta G_d + \sum_{d=1}^{m}\sum_{e=1}^{m}\lambda_{(2)de}^k\delta G_d\delta G_e + \cdots + \underbrace{\sum_{d=1}^{m}\sum_{e=1}^{m}\cdots\sum_{z=1}^{m}}_{p\text{ summations}}\lambda_{(p)de\cdots z}^k\delta G_d\delta G_e\cdots\delta G_z + \varepsilon_\lambda^k \tag{4}$$

$$\overline{\phi}_d^k = \overline{\phi}^k + \sum_{d=1}^{m}\sum_{\substack{a=1\\a\neq k}}^{n} P_{(1)da}^k \overline{\phi}^a \delta G_d + \sum_{d=1}^{m}\sum_{e=1}^{m}\sum_{\substack{b=1\\b\neq k}}^{n} P_{(2)deb}^k \overline{\phi}^b \delta G_d \delta G_e + \cdots + \sum_{d=1}^{m}\sum_{e=1}^{m}\cdots\sum_{z=1}^{m}\sum_{\substack{r=1\\r\neq k}}^{n} P_{(p)de\cdots zr}^k \overline{\phi}^r \delta G_d \delta G_e \cdots \delta G_z + \cdots + \overline{\varepsilon}_\phi^k \tag{5}$$

where $\lambda_{(1)d}^k$, $\lambda_{(2)de}^k$, and $\lambda_{(p)de\cdots z}^k$ are the coefficients of the first, second and p-th order perturbation terms for the eigenvalue. $P_{(1)da}^k$, $P_{(2)deb}^k$ and $P_{(p)de\cdots zr}^k$ are the coefficients of the first, second, and p-th order perturbation terms for the eigenvector. ε_λ^k and $\overline{\varepsilon}_\phi^k$ are the residuals of order $p+1$. In these summation series, running indexes $d, e, \ldots, z = 1, 2, \ldots, m$. Because of the orthogonality relation, one cannot obtain the k-th eigenparameter coefficients by the eigenvalue equation. Using the orthogonality relations of the eigenvectors and substituting perturbation Eq. 5, one can obtain these coefficients through the orthonormal equation:

$$\begin{aligned} 1 &= (\overline{\phi}_d^k)^T M \overline{\phi}_d^k \\ &= \left(\overline{\phi}^k + \sum_{d=1}^{m}\sum_{\substack{a=1\\a\neq k}}^{n} P_{(1)da}^k \overline{\phi}^a \delta G_d + \sum_{d=1}^{m}\sum_{e=1}^{m}\sum_{\substack{b=1\\b\neq k}}^{n} P_{(2)deb}^k \overline{\phi}^b \delta G_d \delta G_e \right. \\ &\quad \left. + \cdots + \sum_{d=1}^{m}\sum_{e=1}^{m}\cdots\sum_{z=1}^{m}\sum_{\substack{r=1\\r\neq k}}^{n} P_{(p)de\cdots zr}^k \overline{\phi}^r \delta G_d \delta G_e \cdots \delta G_z + \cdots \right)^T \\ &\quad \times M \left(\overline{\phi}^k + \sum_{d=1}^{m}\sum_{\substack{a=1\\a\neq k}}^{n} P_{(1)da}^k \overline{\phi}^a \delta G_d + \sum_{d=1}^{m}\sum_{e=1}^{m}\sum_{\substack{b=1\\b\neq k}}^{n} P_{(2)deb}^k \overline{\phi}^b \delta G_d \delta G_e \right. \\ &\quad \left. + \cdots + \sum_{d=1}^{m}\sum_{e=1}^{m}\cdots\sum_{z=1}^{m}\sum_{\substack{r=1\\r\neq k}}^{n} P_{(p)de\cdots zr}^k \overline{\phi}^r \delta G_d \delta G_e \cdots \delta G_z + \cdots \right) \end{aligned} \tag{6}$$

Noting that the L.H.S. of Eq. 6 equals to one and equating the coefficients of the $\delta G_d (d = 1, 2, \ldots, m)$ terms in this orthonormal equation, we have

$$\begin{aligned} 0 &= \overline{\phi}^{kT} M \sum_{a=1}^{n} P_{(1)da}^k \overline{\phi}^a \delta G_d + \sum_{a=1}^{n} P_{(1)da}^k \overline{\phi}^{aT} \delta G_d M \overline{\phi}^k \\ &= 2 \sum_{a=1}^{n} P_{(1)da}^k \overline{\phi}^{kT} M \overline{\phi}^a \delta G_d \end{aligned} \tag{7}$$

by neglecting the residual terms of $\overline{\varepsilon}_\phi^k$. For $a = k$

$$P_{(1)da}^k \overline{\phi}^{kT} M \overline{\phi}^k = 0 \tag{8}$$

and using the orthogonality relation, this implies that the first-order eigenvector coefficient is

$$P_{(1)dk}^k = 0 \tag{9}$$

By equating and simplifying the coefficients of the $\delta G_d \delta G_e (d, e = 1, 2, \ldots, m)$ terms in the orthonormal equation, second-order eigenvector coefficient can be obtained as

$$P^k_{(2)DEk} = \frac{-\mathbb{R}^1_{de}!}{2} \left\{ \frac{1}{1+\tau^e_d} \sum_{\substack{a=1 \\ a\neq k}}^{n} P^k_{(1)da} P^k_{(1)ea} + \frac{1}{1+\tau^d_e} \sum_{\substack{a=1 \\ a\neq k}}^{n} P^k_{(1)ea} P^k_{(1)da} \right\} \tag{10}$$

where τ^e_d is the generalized Kronecker delta defined by

$$\tau^e_d = \begin{cases} 1, & \text{if } d = e \\ 0, & \text{if } d \neq e \end{cases} \tag{11}$$

$\mathbb{R}^1_{de}$ denotes the number of repeated indexes, d and e, in the eigenvalue and eigenvector coefficients, and $\mathbb{R}^1_{de}!$ is the number of all possible permutations of indexes, d and e. Note that the upper case indexes in the subscript of the coefficient indicate that the order of the indexes are not essential. When the eigenvector coefficients are symmetric, the permutation numbers are simplified as the factorial number, i.e. $\mathbb{R}^1_{de} = 2!$. Also $P^k_{(2)DEk} = 2! P^k_{(2)dek}$, therefore Eq. 10 can be rewritten as

$$P^k_{(2)dek} = \frac{-1}{2} \left\{ \frac{1}{1+\tau^e_d} \sum_{\substack{a=1 \\ a\neq k}}^{n} P^k_{(1)da} P^k_{(1)ea} + \frac{1}{1+\tau^d_e} \sum_{\substack{a=1 \\ a\neq k}}^{n} P^k_{(1)ea} P^k_{(1)da} \right\} \tag{12}$$

Similarly, equating and simplifying the coefficients of $\delta G_d \delta G_e \cdots \delta G_z (d, e, \ldots, z = 1, 2, \ldots, m)$ terms yields the p-th order coefficients:

$$\begin{aligned}
P^k_{(p)DE\cdots Zk} = \frac{-\mathbb{R}^1_{de\cdots z}!\mathbb{R}^2_{de\cdots z}! \cdots \mathbb{R}^\alpha_{de\cdots z}!}{2} \Bigg[& \frac{1}{1+\tau^{EF\cdots Z}_d} \sum_{\substack{q=1 \\ q\neq k}}^{n} P^k_{(1)dq} \frac{P^k_{(p-1)EF\cdots Zq}}{\mathbb{R}^1_{ef\cdots z}!\mathbb{R}^2_{ef\cdots z}! \cdots \mathbb{R}^\beta_{ef\cdots z}!} \\
& + \frac{1}{1+\tau^{DF\cdots Z}_e} \sum_{\substack{q=1 \\ q\neq k}}^{n} P^k_{(1)eq} \frac{P^k_{(p-1)DF\cdots Zq}}{\mathbb{R}^1_{df\cdots z}!\mathbb{R}^2_{df\cdots z}! \cdots \mathbb{R}^\chi_{df\cdots z}!} \\
& + \cdots + \frac{1}{1+\tau^{D\cdots XY}_z} \sum_{\substack{q=1 \\ q\neq k}}^{n} P^k_{(1)zq} \frac{P^k_{(p-1)D\cdots XYq}}{\mathbb{R}^1_{d\cdots xy}!\mathbb{R}^2_{d\cdots xy}! \cdots \mathbb{R}^\varphi_{d\cdots xy}!} \\
& + \frac{1}{1+\tau^{F\cdots YZ}_{DE}} \sum_{\substack{q=1 \\ q\neq k}}^{n} \frac{P^k_{(2)DEp}}{\mathbb{R}^1_{de}!} \frac{P^k_{(p-2)F\cdots YZq}}{\mathbb{R}^1_{f\cdots yz}!\mathbb{R}^2_{f\cdots yz}! \cdots \mathbb{R}^\gamma_{f\cdots yz}!} \\
& + \frac{1}{1+\tau^{E\cdots YZ}_{DF}} \sum_{\substack{q=1 \\ q\neq k}}^{n} \frac{P^k_{(2)DFq}}{\mathbb{R}^1_{df}!} \frac{P^k_{(p-2)E\cdots YZq}}{\mathbb{R}^1_{e\cdots yz}!\mathbb{R}^2_{e\cdots yz}! \cdots \mathbb{R}^\eta_{e\cdots yz}!} \\
& + \cdots \frac{1}{1+\tau^{E\cdots XY}_{DZ}} \sum_{\substack{q=1 \\ q\neq k}}^{n} \frac{P^k_{(2)DZq}}{\mathbb{R}^1_{dz}!} \frac{P^k_{(p-2)E\cdots XYq}}{\mathbb{R}^1_{e\cdots xy}!\mathbb{R}^2_{e\cdots xy}! \cdots \mathbb{R}^\kappa_{e\cdots xy}!} \\
& + \frac{1}{1+\tau^{D\cdots YZ}_{EF}} \sum_{\substack{q=1 \\ q\neq k}}^{n} \frac{P^k_{(2)EFq}}{\mathbb{R}^1_{ef}!} \frac{P^k_{(p-2)D\cdots YZq}}{\mathbb{R}^1_{d\cdots yz}!\mathbb{R}^2_{d\cdots yz}! \cdots \mathbb{R}^\mu_{d\cdots yz}!}
\end{aligned}$$

$$
\begin{aligned}
&+\cdots\frac{1}{1+\tau_{EZ}^{D\cdots XY}}\sum_{\substack{q=1\\q\neq k}}^{n}\frac{P_{(2)EZq}^{k}}{\mathbb{R}_{ez}^{1}!}\frac{P_{(p-2)D\cdots XYq}^{k}}{\mathbb{R}_{d\cdots xy}^{1}!\mathbb{R}_{d\cdots xy}^{2}!\cdots\mathbb{R}_{d\cdots xy}^{v}!}\\
&+\cdots+\frac{1}{1+\tau_{YZ}^{DE\cdots X}}\sum_{\substack{q=1\\q\neq k}}^{n}\frac{P_{(2)YZq}^{k}}{\mathbb{R}_{yz}^{1}!}\frac{P_{(p-2)DE\cdots Xq}^{k}}{\mathbb{R}_{de\cdots x}^{1}!\mathbb{R}_{de\cdots x}^{2}!\cdots\mathbb{R}_{de\cdots x}^{\varpi}!}\\
&+\cdots+\frac{1}{1+\tau_{EF\cdots Z}^{d}}\sum_{\substack{q=1\\q\neq k}}^{n}\frac{P_{(p-1)EF\cdots Zq}^{k}}{\mathbb{R}_{ef\cdots z}^{1}!\mathbb{R}_{ef\cdots z}^{2}!\cdots\mathbb{R}_{ef\cdots z}^{\beta}!}P_{(1)dq}^{k}\\
&+\frac{1}{1+\tau_{DF\cdots Z}^{e}}\sum_{\substack{q=1\\q\neq k}}^{n}\frac{P_{(p-1)DF\cdots Zq}^{k}}{\mathbb{R}_{df\cdots z}^{1}!\mathbb{R}_{df\cdots z}^{2}!\cdots\mathbb{R}_{df\cdots z}^{\chi}!}P_{(1)eq}^{k}\\
&+\cdots+\frac{1}{1+\tau_{DE\cdots Y}^{z}}\sum_{\substack{q=1\\q\neq k}}^{n}\frac{P_{(p-1)DE\cdots Yq}^{k}}{\mathbb{R}_{de\cdots y}^{1}!\mathbb{R}_{de\cdots y}^{2}!\cdots\mathbb{R}_{de\cdots y}^{\varphi}!}P_{(1)zq}^{k}\Bigg]
\end{aligned}
\tag{13}
$$

where the generalized Kronecker deltas such as $\tau_{d}^{EF\cdots Z}$ and $\tau_{DE}^{F\cdots YZ}$ are defined by

$$
\tau_{d}^{EF\cdots Z}=\begin{cases}1, & \text{if } d=e,f,\ldots, \text{ or } z\\ 0, & \text{if } d\neq e,f,\ldots, \text{ and } z\end{cases}
\tag{14}
$$

and

$$
\tau_{DE}^{F\cdots YZ}=\begin{cases}1, & \text{if } d \text{ and } e \text{ appear in the indexes in the superscript}\\ 0, & \text{if } \ d \text{ and } e \text{ do not appear in the indexes in the superscript}\end{cases}
\tag{15}
$$

respectively. Note that the upper case indexes in the sub- and superscripts of all the generalized Kronecker deltas in Eqs. 14 and 15 indicate that the orders of the indexes are insignificant. Eigenvector and eigenvalue coefficients such as $P_{(p)DE\cdots Zq}^{k}$ and $\lambda_{(p-1)EF\cdots Z}^{k}$ represent the sums of all terms of the forms $P_{(p)de\cdots z}^{k}$ and $\lambda_{(p-1)ef\cdots z}^{k}$, respectively, with different permutations of indexes $d,e,\ldots z$ and $e,f,\ldots,z$. The coefficients such as $\mathbb{R}_{de\cdots z}^{1},\mathbb{R}_{de\cdots z}^{2},\ldots,\mathbb{R}_{de\cdots z}^{\alpha}$ are the numbers of the first, second and last repeated indexes within indexes $d,e,\ldots,z$. Now assume that the symmetry relation exists, the total value of each coefficient is just one of the coefficients times the factorial of its order. Thus, its symmetric k-th term is

$$
\begin{aligned}
P_{(p)de\cdots zk}^{k}=\frac{-\mathbb{R}_{de\cdots z}^{1}!\mathbb{R}_{de\cdots z}^{2}!\cdots\mathbb{R}_{de\cdots z}^{\alpha}!}{2p!}\Bigg[&\frac{1}{1+\tau_{d}^{EF\cdots Z}}\sum_{\substack{q=1\\q\neq k}}^{n}P_{(1)dq}^{k}\frac{(p-1)!P_{(p-1)ef\cdots zq}^{k}}{\mathbb{R}_{ef\cdots z}^{1}!\mathbb{R}_{ef\cdots z}^{2}!\cdots\mathbb{R}_{ef\cdots z}^{\beta}!}\\
&+\frac{1}{1+\tau_{e}^{DF\cdots Z}}\sum_{\substack{q=1\\q\neq k}}^{n}P_{(1)eq}^{k}\frac{(p-1)!P_{(p-1)df\cdots zq}^{k}}{\mathbb{R}_{df\cdots z}^{1}!\mathbb{R}_{df\cdots z}^{2}!\cdots\mathbb{R}_{df\cdots z}^{\chi}!}\\
&+\cdots+\frac{1}{1+\tau_{z}^{D\cdots XY}}\sum_{\substack{q=1\\q\neq k}}^{n}P_{(1)zq}^{k}\frac{(p-1)!P_{(p-1)d\cdots xyq}^{k}}{\mathbb{R}_{d\cdots xy}^{1}!\mathbb{R}_{d\cdots xy}^{2}!\cdots\mathbb{R}_{d\cdots xy}^{\varphi}!}\\
&+\frac{1}{1+\tau_{DE}^{F\cdots YZ}}\sum_{\substack{q=1\\q\neq k}}^{n}\frac{2!P_{(2)deq}^{k}}{\mathbb{R}_{de}^{1}!}\frac{(p-2)!P_{(p-2)f\cdots yzq}^{k}}{\mathbb{R}_{f\cdots yz}^{1}!\mathbb{R}_{f\cdots yz}^{2}!\cdots\mathbb{R}_{f\cdots yz}^{\gamma}!}
\end{aligned}
$$

$$
\begin{aligned}
&+\frac{1}{1+\tau_{DF}^{E\cdots YZ}}\sum_{\substack{q=1\\q\neq k}}^{n}\frac{2!P_{(2)dfq}^{k}}{\mathbb{R}_{df}^{1}!}\frac{(p-2)!P_{(p-2)e\cdots yzq}^{k}}{\mathbb{R}_{e\cdots yz}^{1}!\mathbb{R}_{e\cdots yz}^{2}!\cdots\mathbb{R}_{e\cdots yz}^{\eta}!}\\
&+\cdots\frac{1}{1+\tau_{DZ}^{E\cdots XY}}\sum_{\substack{q=1\\q\neq k}}^{n}\frac{2!P_{(2)dzq}^{k}}{\mathbb{R}_{dz}^{1}!}\frac{(p-2)!P_{(p-2)e\cdots xyq}^{k}}{\mathbb{R}_{e\cdots xy}^{1}!\mathbb{R}_{e\cdots xy}^{2}!\cdots\mathbb{R}_{e\cdots xy}^{\kappa}!}\\
&+\frac{1}{1+\tau_{EF}^{D\cdots YZ}}\sum_{\substack{q=1\\q\neq k}}^{n}\frac{2!P_{(2)efq}^{k}}{\mathbb{R}_{ef}^{1}!}\frac{(p-2)!P_{(p-2)d\cdots yzq}^{k}}{\mathbb{R}_{d\cdots yz}^{1}!\mathbb{R}_{d\cdots yz}^{2}!\cdots\mathbb{R}_{d\cdots yz}^{\mu}!}\\
&+\cdots\frac{1}{1+\tau_{EZ}^{D\cdots XY}}\sum_{\substack{q=1\\q\neq k}}^{n}\frac{2!P_{(2)ezq}^{k}}{\mathbb{R}_{ez}^{1}!}\frac{(p-2)!P_{(p-2)d\cdots xyq}^{k}}{\mathbb{R}_{d\cdots xy}^{1}!\mathbb{R}_{d\cdots xy}^{2}!\cdots\mathbb{R}_{d\cdots xy}^{\nu}!}\\
&+\cdots+\frac{1}{1+\tau_{YZ}^{DE\cdots X}}\sum_{\substack{q=1\\q\neq k}}^{n}\frac{2!P_{(2)yzq}^{k}}{\mathbb{R}_{yz}^{1}!}\frac{(p-2)!P_{(p-2)de\cdots xq}^{k}}{\mathbb{R}_{de\cdots x}^{1}!\mathbb{R}_{de\cdots x}^{2}!\cdots\mathbb{R}_{de\cdots x}^{\varpi}!}\\
&+\cdots+\frac{1}{1+\tau_{EF\cdots Z}^{d}}\sum_{\substack{q=1\\q\neq k}}^{n}\frac{(p-1)!P_{(p-1)ef\cdots zq}^{k}}{\mathbb{R}_{ef\cdots z}^{1}!\mathbb{R}_{ef\cdots z}^{2}!\cdots\mathbb{R}_{ef\cdots z}^{\beta}!}P_{(1)dq}^{k}\\
&+\frac{1}{1+\tau_{DF\cdots Z}^{e}}\sum_{\substack{q=1\\q\neq k}}^{n}\frac{(p-1)!P_{(p-1)df\cdots zq}^{k}}{\mathbb{R}_{df\cdots z}^{1}!\mathbb{R}_{df\cdots z}^{2}!\cdots\mathbb{R}_{df\cdots z}^{\chi}!}P_{(1)eq}^{k}\\
&+\cdots+\frac{1}{1+\tau_{DE\cdots Y}^{z}}\sum_{\substack{q=1\\q\neq k}}^{n}\frac{(p-1)!P_{(p-1)de\cdots yq}^{k}}{\mathbb{R}_{de\cdots y}^{1}!\mathbb{R}_{de\cdots y}^{2}!\cdots\mathbb{R}_{de\cdots y}^{\varphi}!}P_{(1)zq}^{k}\Bigg]
\end{aligned}
\tag{16}
$$

On the other hand, we consider the terms other than the k-th term by substituting perturbed λ_d^k, $\overline{\phi}_d^k$ and K_d into Eq. 2 of the damaged structure to get the perturbed eigenvalue equation of the damaged structure. Different order perturbation terms in the equation can be derived by equating the coefficients of like order terms of δG_d. Equating the coefficients of the $\delta G_d (d = 1, 2, \ldots, m)$ terms yields

$$
K\sum_{\substack{a=1\\a\neq k}}^{n}P_{(1)da}^{k}\overline{\phi}^{a}+\frac{\partial K}{\partial G_d}\overline{\phi}^{k}=\lambda^{k}M\sum_{\substack{a=1\\a\neq k}}^{n}P_{(1)da}^{k}\overline{\phi}^{a}+\lambda_{(1)d}^{k}M\overline{\phi}^{k} \tag{17}
$$

To obtain the eigenvalue coefficients by premultiplying Eq. 17 by $\overline{\phi}^{kT}$, then using Eq. 1 and the orthonormal relations yields

$$
\lambda_{(1)d}^{k}=\overline{\phi}^{kT}\frac{\partial K}{\partial G_d}\overline{\phi}^{k} \tag{18}
$$

On the other hand, the eigenvector coefficients can be obtained by premultiplying Eq. 17 by $\overline{\phi}^{gT}$, where $g \neq k$, one gets

$$
\sum_{\substack{a=1\\a\neq k}}^{n}P_{(1)da}^{k}\overline{\phi}^{gT}K\overline{\phi}^{a}+\overline{\phi}^{gT}\frac{\partial K}{\partial G_d}\overline{\phi}^{k}=\lambda^{k}\sum_{\substack{a=1\\a\neq k}}^{n}P_{(1)da}^{k}\overline{\phi}^{gT}M\overline{\phi}^{a}+\lambda_{(1)d}^{k}\overline{\phi}^{gT}M\overline{\phi}^{k} \tag{19}
$$

Use of Eq. 1, we get $K\overline{\phi}^g = \lambda^g M\overline{\phi}^g$, and the orthonormal relations in Eq. 19 yield

$$P^k_{(1)dg} = \frac{1}{\lambda^k - \lambda^g}\left\{\overline{\phi}^{gT}\frac{\partial K}{\partial G_d}\overline{\phi}^k\right\} \tag{20}$$

Equating the coefficients of the $\delta G_d \delta G_e (d, e = 1, 2, \ldots, m)$ terms in the perturbed eigenvalue equation of the damaged structure, one can obtain

$$\begin{aligned}
&\frac{1}{\mathbb{R}^1_{de}!}K\sum_{\substack{b=1\\b\neq k}}^{n}P^k_{(2)deb}\overline{\phi}^b + \frac{1}{\mathbb{R}^1_{de}!}K\sum_{\substack{b=1\\b\neq k}}^{n}P^k_{(2)edb}\overline{\phi}^b + \frac{1}{1+\tau^e_d}\left[\frac{\partial K}{\partial G_d}\sum_{\substack{a=1\\a\neq k}}^{n}P^k_{(1)ea}\overline{\phi}^a\right]\\
&+\frac{1}{1+\tau^d_e}\left[\frac{\partial K}{\partial G_e}\sum_{\substack{a=1\\a\neq k}}^{n}P^k_{(1)da}\overline{\phi}^a\right] = \frac{1}{\mathbb{R}^1_{de}!}\lambda^k M\sum_{\substack{b=1\\b\neq k}}^{n}P^k_{(2)deb}\overline{\phi}^b + \frac{1}{\mathbb{R}^1_{de}!}\lambda^k M\sum_{\substack{b=1\\b\neq k}}^{n}P^k_{(2)edb}\overline{\phi}^b\\
&+\frac{1}{1+\tau^e_d}\left[\lambda^k_{(1)d}M\sum_{\substack{a=1\\a\neq k}}^{n}P^k_{(1)ea}\overline{\phi}^a\right] + \frac{1}{1+\tau^d_e}\left[\lambda^k_{(1)e}M\sum_{\substack{a=1\\a\neq k}}^{n}P^k_{(1)da}\overline{\phi}^a\right] + \frac{1}{\mathbb{R}^1_{de}!}\lambda^k_{(2)de}M\overline{\phi}^k\\
&+\frac{1}{\mathbb{R}^1_{de}!}\lambda^k_{(2)ed}M\overline{\phi}^k
\end{aligned} \tag{21}$$

where τ^e_d is the generalized Kronecker delta defined by Eq. 11. Consider the eigenvalue coefficients by premultiplying Eq. 21 by $\overline{\phi}^{kT}$, and through the use of orthonormal relations, generalized Kronecker deltas and permutation numbers,it is reduced to

$$\lambda^k_{(2)DE} = \mathbb{R}^1_{de}!\left(\frac{1}{1+\tau^e_d}\sum_{\substack{a=1\\a\neq k}}^{n}P^k_{(1)ea}\overline{\phi}^{kT}\frac{\partial K}{\partial G_d}\overline{\phi}^a + \frac{1}{1+\tau^d_e}\sum_{\substack{a=1\\a\neq k}}^{n}P^k_{(1)da}\overline{\phi}^{kT}\frac{\partial K}{\partial G_e}\overline{\phi}^a\right) \tag{22}$$

where $\lambda^k_{(2)DE}$ denotes all combination of $\lambda^k_{(2)de}$, i.e.$\lambda^k_{(2)DE} = \lambda^k_{(2)de} + \lambda^k_{(2)ed}$. Note that the upper case indexes in the subscript of the coefficient indicate that the order of the indexes is not essential. When the second-order eigenvalue coefficient is symmetric, the permutation number is simplified as the factorial number, i.e. $\mathbb{R}^1_{de} = 2!$. Eq. 22 can be rewritten as

$$\lambda^k_{(2)de} = \frac{1}{1+\tau^e_d}\sum_{\substack{a=1\\a\neq k}}^{n}P^k_{(1)ea}\overline{\phi}^{kT}\frac{\partial K}{\partial G_d}\overline{\phi}^a + \frac{1}{1+\tau^d_e}\sum_{\substack{a=1\\a\neq k}}^{n}P^k_{(1)da}\overline{\phi}^{kT}\frac{\partial K}{\partial G_e}\overline{\phi}^a \tag{23}$$

Consider the eigenvector coefficients by premultiplying Eq. 21 by $\overline{\phi}^{hT}$, where $h \neq k$. Through the use of Eq. 1, and the orthonormal relations, it is reduced to

$$\begin{aligned}
&\frac{1}{\mathbb{R}^1_{de}!}\lambda^h P^k_{(2)deh} + \frac{1}{\mathbb{R}^1_{de}!}\lambda^h P^k_{(2)edh} + \frac{1}{1+\tau^e_d}\sum_{\substack{a=1\\a\neq k}}^{n}P^k_{(1)ea}\overline{\phi}^{hT}\frac{\partial K}{\partial G_d}\overline{\phi}^a + \frac{1}{1+\tau^d_e}\sum_{\substack{a=1\\a\neq k}}^{n}P^k_{(1)da}\overline{\phi}^{hT}\frac{\partial K}{\partial G_e}\overline{\phi}^a\\
&= \frac{1}{\mathbb{R}^1_{de}!}\lambda^k P^k_{(2)deh} + \frac{1}{\mathbb{R}^1_{de}!}\lambda^k P^k_{(2)edh} + \frac{1}{1+\tau^e_d}\lambda^k_{(1)d}P^k_{(1)eh} + \frac{1}{1+\tau^d_e}\lambda^k_{(1)e}P^k_{(1)dh}
\end{aligned} \tag{24}$$

Simplifying Eq. 24, one can get

$$P^k_{(2)DEh} = \frac{\mathbb{R}^1_{de}!}{\lambda^k - \lambda^h}\left(\frac{1}{1+\tau^e_d}\sum_{\substack{a=1\\a\neq k}}^{n} P^k_{(1)ea}\overline{\phi}^{hT}\frac{\partial K}{\partial G_d}\overline{\phi}^a + \frac{1}{1+\tau^d_e}\sum_{\substack{a=1\\a\neq k}}^{n} P^k_{(1)da}\overline{\phi}^{hT}\frac{\partial K}{\partial G_e}\overline{\phi}^a - \frac{1}{1+\tau^e_d}\lambda^k_{(1)d}P^k_{(1)eh} - \frac{1}{1+\tau^d_e}\lambda^k_{(1)e}P^k_{(1)dh}\right) \tag{25}$$

where $P^k_{(2)DE}$ denotes all combination of $P^k_{(2)de}$, i.e. $P^k_{(2)DE} = P^k_{(2)de} + P^k_{(2)ed}$. For the symmetric second-order eigenvector coefficient, its total numbers are the factorial numbers of its order. Also, the permutation number is same as the factorial number, i.e. $\mathbb{R}^1_{de} = 2!$. Therefore Eq. 25 can be rewritten as:

$$P^k_{(2)edh} = \frac{1}{\lambda^k - \lambda^h}\left(\frac{1}{1+\tau^e_d}\sum_{\substack{a=1\\a\neq k}}^{n} P^k_{(1)ea}\overline{\phi}^{hT}\frac{\partial K}{\partial G_d}\overline{\phi}^a + \frac{1}{1+\tau^d_e}\sum_{\substack{a=1\\a\neq k}}^{n} P^k_{(1)da}\overline{\phi}^{hT}\frac{\partial K}{\partial G_e}\overline{\phi}^a - \frac{1}{1+\tau^e_d}\lambda^k_{(1)d}P^k_{(1)eh} - \frac{1}{1+\tau^d_e}\lambda^k_{(1)e}P^k_{(1)dh}\right) \tag{26}$$

Now we can proceed to find the eigenvalue and eigenvector coefficients for the p-th order terms. Consider here the case with $m \geq p$. Equating the coefficients of the $\delta G_d \delta G_e \cdots \delta G_z (d, e, \ldots, z = 1, 2, \ldots, m)$ terms in perturbed eigenvalue equation results in

$$\begin{aligned}
&K\sum_{\substack{r=1\\r\neq k}}^{n}\frac{P^k_{(p)DE\cdots Zr}}{\mathbb{R}^1_{de\cdots z}!\mathbb{R}^2_{de\cdots z}!\cdots\mathbb{R}^{\alpha}_{de\cdots z}!}\overline{\phi}^r + \frac{1}{1+\tau^{EF\cdots Z}_d}\frac{\partial K}{\partial G_d}\sum_{\substack{q=1\\q\neq k}}^{n}\frac{P^k_{(p-1)EF\cdots Zq}}{\mathbb{R}^1_{ef\cdots z}!\mathbb{R}^2_{ef\cdots z}!\cdots\mathbb{R}^{\beta}_{ef\cdots z}!}\overline{\phi}^q \\
&\quad + \frac{1}{1+\tau^{DF\cdots Z}_e}\frac{\partial K}{\partial G_e}\sum_{\substack{q=1\\q\neq k}}^{n}\frac{P^k_{(p-1)DF\cdots Zq}}{\mathbb{R}^1_{df\cdots z}!\mathbb{R}^2_{df\cdots z}!\cdots\mathbb{R}^{\chi}_{df\cdots z}!}\overline{\phi}^q \\
&\quad + \cdots + \frac{1}{1+\tau^{DE\cdots Y}_z}\frac{\partial K}{\partial G_z}\sum_{\substack{q=1\\q\neq k}}^{n}\frac{P^k_{(p-1)D\cdots XYq}}{\mathbb{R}^1_{d\cdots xy}!\mathbb{R}^2_{d\cdots xy}!\cdots\mathbb{R}^{\varphi}_{de\cdots xy}!}\overline{\phi}^q \\
&= \lambda^k M\sum_{\substack{r=1\\r\neq k}}^{n}\frac{P^k_{(p)DE\cdots Zr}}{\mathbb{R}^1_{de\cdots z}!\mathbb{R}^2_{de\cdots z}!\cdots\mathbb{R}^{\alpha}_{de\cdots z}!}\overline{\phi}^r \\
&\quad + \frac{\lambda^k_{(1)d}}{1+\tau^{EF\cdots Z}_d}M\sum_{\substack{q=1\\q\neq k}}^{n}\frac{P^k_{(p-1)EF\cdots Zq}}{\mathbb{R}^1_{ef\cdots z}!\mathbb{R}^2_{ef\cdots z}!\cdots\mathbb{R}^{\beta}_{ef\cdots z}!}\overline{\phi}^q \\
&\quad + \frac{\lambda^k_{(1)e}}{1+\tau^{DF\cdots Z}_e}M\sum_{\substack{q=1\\q\neq k}}^{n}\frac{P^k_{(p-1)DF\cdots Zq}}{\mathbb{R}^1_{df\cdots z}!\mathbb{R}^2_{df\cdots z}!\cdots\mathbb{R}^{\chi}_{df\cdots z}!}\overline{\phi}^q \\
&\quad + \cdots + \frac{\lambda^k_{(1)z}}{1+\tau^{D\cdots XY}_z}M\sum_{\substack{q=1\\q\neq k}}^{n}\frac{P^k_{(p-1)D\cdots XYq}}{\mathbb{R}^1_{d\cdots xy}!\mathbb{R}^2_{d\cdots xy}!\cdots\mathbb{R}^{\varphi}_{d\cdots xy}!}\overline{\phi}^q
\end{aligned}$$

$$
\begin{aligned}
&+\frac{\lambda^k_{(2)DE}}{\mathbb{R}^1_{de}!\left(1+\tau^{F\cdots YZ}_{DE}\right)}M\sum_{\substack{p=1\\p\neq k}}^{n}\frac{P^k_{(p-2)F\cdots YZp}}{\mathbb{R}^1_{f\cdots yz}!\mathbb{R}^2_{f\cdots yz}!\cdots\mathbb{R}^{\gamma}_{f\cdots yz}!}\overline{\phi}^p\\
&+\frac{\lambda^k_{(2)DF}}{\mathbb{R}^1_{df}!\left(1+\tau^{E\cdots YZ}_{DF}\right)}M\sum_{\substack{p=1\\p\neq k}}^{n}\frac{P^k_{(p-2)E\cdots YZp}}{\mathbb{R}^1_{e\cdots yz}!\mathbb{R}^2_{e\cdots yz}!\cdots\mathbb{R}^{\eta}_{e\cdots yz}!}\overline{\phi}^p\\
&+\cdots\frac{\lambda^k_{(2)DZ}}{\mathbb{R}^1_{dz}!\left(1+\tau^{E\cdots XY}_{DZ}\right)}M\sum_{\substack{p=1\\p\neq k}}^{n}\frac{P^k_{(p-2)E\cdots XYp}}{\mathbb{R}^1_{e\cdots xy}!\mathbb{R}^2_{e\cdots xy}!\cdots\mathbb{R}^{\kappa}_{e\cdots xy}!}\overline{\phi}^p\\
&+\frac{\lambda^k_{(2)EF}}{\mathbb{R}^1_{ef}!\left(1+\tau^{D\cdots YZ}_{EF}\right)}M\sum_{\substack{p=1\\p\neq k}}^{n}\frac{P^k_{(p-2)D\cdots YZp}}{\mathbb{R}^{\phi 1}_{d\cdots yz}!\mathbb{R}^{\phi 2}_{d\cdots yz}!\cdots\mathbb{R}^{\mu}_{d\cdots yz}!}\overline{\phi}^p\\
&+\cdots\frac{\lambda^k_{(2)EZ}}{\mathbb{R}^1_{ez}!\left(1+\tau^{D\cdots XY}_{EZ}\right)}M\sum_{\substack{p=1\\p\neq k}}^{n}\frac{P^k_{(p-2)D\cdots XYp}}{\mathbb{R}^1_{d\cdots xy}!\mathbb{R}^2_{d\cdots xy}!\cdots\mathbb{R}^{\nu}_{d\cdots xy}!}\overline{\phi}^p\\
&+\cdots+\frac{\lambda^k_{(2)YZ}}{\mathbb{R}^1_{yz}!\left(1+\tau^{DE\cdots X}_{YZ}\right)}M\sum_{\substack{p=1\\p\neq k}}^{n}\frac{P^k_{(p-2)DE\cdots Xp}}{\mathbb{R}^1_{de\cdots x}!\mathbb{R}^2_{de\cdots x}!\cdots\mathbb{R}^{\varpi}_{de\cdots x}!}\overline{\phi}^p\\
&+\cdots+\frac{\lambda^k_{(p-1)EF\cdots Z}}{\mathbb{R}^1_{ef\cdots z}!\mathbb{R}^2_{ef\cdots z}!\cdots\mathbb{R}^{\beta}_{ef\cdots z}!\left(1+\tau^{d}_{EF\cdots Z}\right)}M\sum_{\substack{a=1\\a\neq k}}^{n}P^k_{(1)da}\overline{\phi}^a\\
&+\frac{\lambda^k_{(p-1)DF\cdots Z}}{\mathbb{R}^1_{df\cdots z}!\mathbb{R}^2_{df\cdots z}!\cdots\mathbb{R}^{x}_{df\cdots z}!\left(1+\tau^{\chi}_{DF\cdots Z}\right)}M\sum_{\substack{a=1\\a\neq k}}^{n}P^k_{(1)ea}\overline{\phi}^a\\
&+\cdots+\frac{\lambda^k_{(p-1)DE\cdots Y}}{\mathbb{R}^1_{de\cdots y}!\mathbb{R}^2_{de\cdots y}!\cdots\mathbb{R}^{\varphi}_{de\cdots y}!\left(1+\tau^{z}_{DE\cdots Y}\right)}M\sum_{\substack{a=1\\a\neq k}}^{n}P^k_{(1)za}\overline{\phi}^a+\frac{\lambda^k_{(p)DE\cdots Z}}{\mathbb{R}^1_{de\cdots z}!\mathbb{R}^2_{de\cdots z}!\cdots\mathbb{R}^{\alpha}_{de\cdots z}!}M\overline{\phi}^k.
\end{aligned}
\tag{27}
$$

where the generalized Kronecker deltas such as $\tau^{EF\cdots Z}_{d}$ and $\tau^{F\cdots YZ}_{DE}$ are defined by Eqs. 14 and 15 as before. Premultiplying Eq. 27 by $\overline{\phi}^{kT}$ and using Eq. 1 and the orthonormal relations in the resulting equation, one can obtain

$$
\begin{aligned}
\lambda^k_{(p)DE\cdots Z}=\mathbb{R}^1_{de\cdots n}!\mathbb{R}^2_{de\cdots n}!\cdots\mathbb{R}^{\alpha}_{de\cdots n}!\Bigg(&\frac{1}{1+\tau^{EF\cdots Z}_{d}}\sum_{\substack{q=1\\q\neq k}}^{n}\frac{P^k_{(p-1)EF\cdots Zq}}{\mathbb{R}^1_{ef\cdots z}!\mathbb{R}^2_{ef\cdots z}!\cdots\mathbb{R}^{\beta}_{ef\cdots z}!}\overline{\phi}^{kT}\frac{\partial K}{\partial G_d}\overline{\phi}^q\\
&+\frac{1}{1+\tau^{DF\cdots Z}_{e}}\sum_{\substack{q=1\\q\neq k}}^{n}\frac{P^k_{(p-1)DF\cdots Zq}}{\mathbb{R}^1_{df\cdots z}!\mathbb{R}^2_{df\cdots z}!\cdots\mathbb{R}^{\chi}_{df\cdots z}!}\overline{\phi}^{kT}\frac{\partial K}{\partial G_e}\overline{\phi}^q\\
&+\cdots+\frac{1}{1+\tau^{DE\cdots Y}_{z}}\sum_{\substack{q=1\\q\neq k}}^{n}\frac{P^k_{(p-1)DE\cdots Yq}}{\mathbb{R}^1_{de\cdots y}!\mathbb{R}^2_{de\cdots y}!\cdots\mathbb{R}^{\varphi}_{de\cdots y}!}\overline{\phi}^{kT}\frac{\partial K}{\partial G_z}\overline{\phi}^q\Bigg)
\end{aligned}
\tag{28}
$$

where $\lambda^k_{(p)DE\cdots Z}$ denotes all combination of $\lambda^k_{(p)de\cdots z}$, i.e.$\lambda^k_{(p)DE\cdots Z} = \lambda^k_{(p)de\cdots z} + \lambda^k_{(p)ed\cdots z} + \cdots + \lambda^k_{(p)d\cdots yz}$. When the eigenparameter coefficients are symmetric, their total numbers are the factorial numbers of their orders, e.g. $\lambda^k_{(p)DE\cdots Z} = p!\lambda^k_{(p)de\cdots z}$. So the p-th order eigenvalue coefficient is reduced to

$$\begin{aligned}\lambda^k_{(p)de\cdots z} = \frac{\mathbb{R}^1_{de\cdots n}!\mathbb{R}^2_{de\cdots n}!\cdots\mathbb{R}^{\alpha}_{de\cdots n}!}{p!}\Bigg(&\frac{1}{1+\tau_d^{EF\cdots Z}}\sum_{\substack{q=1\\q\neq k}}^{n}\frac{(p-1)!P^k_{(p-1)ef\cdots zq}}{\mathbb{R}^1_{ef\cdots z}!\mathbb{R}^2_{ef\cdots z}!\cdots\mathbb{R}^{\beta}_{ef\cdots z}!}\overline{\phi}^{kT}\frac{\partial K}{\partial G_d}\overline{\phi}^{q}\\ &+\frac{1}{1+\tau_e^{DF\cdots Z}}\sum_{\substack{q=1\\q\neq k}}^{n}\frac{(p-1)!P^k_{(p-1)df\cdots zq}}{\mathbb{R}^1_{df\cdots z}!\mathbb{R}^2_{df\cdots z}!\cdots\mathbb{R}^{\chi}_{df\cdots z}!}\overline{\phi}^{kT}\frac{\partial K}{\partial G_e}\overline{\phi}^{q}\\ &+\cdots+\frac{1}{1+\tau_z^{DE\cdots Y}}\sum_{\substack{q=1\\q\neq k}}^{n}\frac{(p-1)!P^k_{(p-1)de\cdots yq}}{\mathbb{R}^1_{de\cdots y}!\mathbb{R}^2_{de\cdots y}!\cdots\mathbb{R}^{\varphi}_{de\cdots y}!}\overline{\phi}^{kT}\frac{\partial K}{\partial G_z}\overline{\phi}^{q}\Bigg)\end{aligned} \tag{29}$$

Premultiplying Eq. 27 by $\overline{\phi}^{wT}$, where $w \neq k$, and using Eq. 1 and the orthonormal relations yield the generalized-order skew-symmetric non k-th term eigenvector coefficient

$$\begin{aligned}P^k_{(p)DE\cdots Zw} = \frac{\mathbb{R}^1_{de\cdots z}!\mathbb{R}^2_{de\cdots z}!\cdots\mathbb{R}^{x}_{de\cdots z}!}{\lambda^k-\lambda^w}\Bigg[&\frac{1}{1+\tau_d^{EF\cdots Z}}\sum_{\substack{q=1\\q\neq k}}^{n}\frac{P^k_{(p-1)EF\cdots Zq}}{\mathbb{R}^1_{ef\cdots z}!\mathbb{R}^2_{ef\cdots z}!\cdots\mathbb{R}^{\beta}_{ef\cdots z}!}\overline{\phi}^{wT}\frac{\partial K}{\partial G_d}\overline{\phi}^{q}\\ &+\frac{1}{1+\tau_e^{DF\cdots Z}}\sum_{\substack{q=1\\q\neq k}}^{n}\frac{P^k_{(p-1)DF\cdots Zq}}{\mathbb{R}^1_{df\cdots z}!\mathbb{R}^2_{df\cdots z}!\cdots\mathbb{R}^{\chi}_{df\cdots z}!}\overline{\phi}^{wT}\frac{\partial K}{\partial G_e}\overline{\phi}^{q}\\ &+\cdots+\frac{1}{1+\tau_z^{DE\cdots Y}}\sum_{\substack{q=1\\q\neq k}}^{n}\frac{P^k_{(p-1)DE\cdots Yq}}{\mathbb{R}^1_{de\cdots y}!\mathbb{R}^2_{de\cdots y}!\cdots\mathbb{R}^{\varphi}_{de\cdots y}!}\overline{\phi}^{wT}\frac{\partial K}{\partial G_z}\overline{\phi}^{q}\\ &-\frac{\lambda^k_{(1)d}}{1+\tau_d^{EF\cdots Z}}\frac{P^k_{(p-1)EF\cdots Zw}}{\mathbb{R}^1_{ef\cdots z}!\mathbb{R}^2_{ef\cdots z}!\cdots\mathbb{R}^{\beta}_{ef\cdots z}!}\\ &-\frac{\lambda^k_{(1)e}}{1+\tau_e^{DF\cdots Z}}\frac{P^k_{(p-1)DF\cdots Zw}}{\mathbb{R}^1_{df\cdots z}!\mathbb{R}^2_{df\cdots z}!\cdots\mathbb{R}^{\chi}_{df\cdots z}!}\\ &-\cdots-\frac{\lambda^k_{(1)z}}{1+\tau_n^{D\cdots XY}}\frac{P^k_{(p-1)D\cdots XYw}}{\mathbb{R}^1_{d\cdots xy}!\mathbb{R}^2_{d\cdots xy}!\cdots\mathbb{R}^{\varphi}_{d\cdots xy}!}-\frac{\lambda^k_{(2)DE}}{\mathbb{R}^1_{de}!\left(1+\tau_{DE}^{F\cdots YZ}\right)}\frac{P^k_{(p-2)F\cdots YZw}}{\mathbb{R}^1_{f\cdots yz}!\mathbb{R}^2_{f\cdots yz}!\cdots\mathbb{R}^{\gamma}_{f\cdots yz}!}\\ &-\frac{\lambda^k_{(2)DF}}{\mathbb{R}^1_{df}!\left(1+\tau_{DF}^{E\cdots MN}\right)}\frac{P^k_{(p-2)E\cdots MNw}}{\mathbb{R}^1_{e\cdots mn}!\mathbb{R}^2_{e\cdots mn}!\cdots\mathbb{R}^{\eta}_{e\cdots mn}!}\\ &-\cdots-\frac{\lambda^k_{(2)DN}}{\mathbb{R}^1_{dn}!\left(1+\tau_{DN}^{E\cdots LM}\right)}\frac{P^k_{(p-2)E\cdots LMw}}{\mathbb{R}^1_{e\cdots lm}!\mathbb{R}^2_{e\cdots lm}!\cdots\mathbb{R}^{\kappa}_{e\cdots lm}!}\\ &-\frac{\lambda^k_{(2)EF}}{\mathbb{R}^1_{ef}!\left(1+\tau_{EF}^{D\cdots MN}\right)}\frac{P^k_{(p-2)D\cdots MNw}}{\mathbb{R}^{\phi 1}_{d\cdots mn}!\mathbb{R}^{\phi 2}_{d\cdots mn}!\cdots\mathbb{R}^{\mu}_{d\cdots mn}!}\\ &-\cdots-\frac{\lambda^k_{(2)EN}}{\mathbb{R}^1_{en}!\left(1+\tau_{EN}^{D\cdots LM}\right)}\frac{P^k_{(p-2)D\cdots LMw}}{\mathbb{R}^1_{d\cdots lm}!\mathbb{R}^2_{d\cdots lm}!\cdots\mathbb{R}^{\nu}_{d\cdots lm}!}\end{aligned}$$

$$
\begin{aligned}
&-\cdots-\frac{\lambda^k_{(2)MN}}{\mathbb{R}^1_{mn}!\left(1+\tau^{DE\cdots L}_{MN}\right)}\frac{P^k_{(p-2)DE\cdots Lw}}{\mathbb{R}^1_{de\cdots l}!\mathbb{R}^2_{de\cdots l}!\cdots\mathbb{R}^{\varpi}_{de\cdots l}!}\\
&-\cdots-\frac{\lambda^k_{(p-1)EF\cdots N}}{\mathbb{R}^1_{ef\cdots n}!\mathbb{R}^2_{ef\cdots n}!\cdots\mathbb{R}^{\beta}_{ef\cdots n}!\left(1+\tau^{d}_{EF\cdots N}\right)}P^k_{(1)dw}-\frac{\lambda^k_{(p-1)DF\cdots N}}{\mathbb{R}^1_{df\cdots n}!\mathbb{R}^2_{df\cdots n}!\cdots\mathbb{R}^{\chi}_{df\cdots n}!\left(1+\tau^{e}_{DF\cdots N}\right)}P^k_{(1)ew}\\
&-\cdots-\frac{\lambda^k_{(p-1)DE\cdots M}}{\mathbb{R}^1_{de\cdots m}!\mathbb{R}^2_{de\cdots m}!\cdots\mathbb{R}^{\varphi}_{de\cdots m}!\left(1+\tau^{z}_{DE\cdots M}\right)}P^k_{(1)nw}\Bigg]
\end{aligned}
\tag{30}
$$

Now consider that the eigenparameter coefficients are symmetric, their total numbers are the factorial numbers of their orders. Therefore, the p-th order symmetric non k-th term eigenvector coefficient can be rewritten as

$$
\begin{aligned}
P^k_{(p)de\cdots zw}=\frac{\mathbb{R}^1_{de\cdots z}!\mathbb{R}^2_{de\cdots z}!\cdots\mathbb{R}^{x}_{de\cdots z}!}{p!\left(\lambda^k-\lambda^w\right)}\Bigg[&\frac{1}{1+\tau^{EF\cdots Z}_{d}}\sum_{\substack{q=1\\q\neq k}}^{n}\frac{(p-1)!P^k_{(p-1)ef\cdots zq}}{\mathbb{R}^1_{ef\cdots z}!\mathbb{R}^2_{ef\cdots z}!\cdots\mathbb{R}^{\beta}_{ef\cdots z}!}\overline{\phi}^{wT}\frac{\partial K}{\partial G_d}\overline{\phi}^{q}\\
+&\frac{1}{1+\tau^{DF\cdots Z}_{e}}\sum_{\substack{q=1\\q\neq k}}^{n}\frac{(p-1)!P^k_{(p-1)df\cdots zq}}{\mathbb{R}^1_{df\cdots z}!\mathbb{R}^2_{df\cdots z}!\cdots\mathbb{R}^{\chi}_{df\cdots z}!}\overline{\phi}^{wT}\frac{\partial K}{\partial G_e}\overline{\phi}^{q}\\
+\cdots+&\frac{1}{1+\tau^{DE\cdots Y}_{z}}\sum_{\substack{q=1\\q\neq k}}^{n}\frac{(p-1)!P^k_{(p-1)de\cdots yq}}{\mathbb{R}^1_{de\cdots y}!\mathbb{R}^2_{de\cdots y}!\cdots\mathbb{R}^{\varphi}_{de\cdots y}!}\overline{\phi}^{wT}\frac{\partial K}{\partial G_z}\overline{\phi}^{q}\\
-&\frac{\lambda^k_{(1)d}}{1+\tau^{EF\cdots Z}_{d}}\frac{(p-1)!P^k_{(p-1)ef\cdots zw}}{\mathbb{R}^1_{ef\cdots z}!\mathbb{R}^2_{ef\cdots z}!\cdots\mathbb{R}^{\beta}_{ef\cdots z}!}-\frac{\lambda^k_{(1)e}}{1+\tau^{DF\cdots Z}_{e}}\frac{(p-1)!P^k_{(p-1)df\cdots zw}}{\mathbb{R}^1_{df\cdots z}!\mathbb{R}^2_{df\cdots z}!\cdots\mathbb{R}^{\chi}_{df\cdots z}!}\\
-\cdots-&\frac{\lambda^k_{(1)z}}{1+\tau^{D\cdots XY}_{n}}\frac{(p-1)!P^k_{(p-1)d\cdots xyw}}{\mathbb{R}^1_{d\cdots xy}!\mathbb{R}^2_{d\cdots xy}!\cdots\mathbb{R}^{\varphi}_{d\cdots xy}!}-\frac{2!\lambda^k_{(2)de}}{\mathbb{R}^1_{de}!\left(1+\tau^{F\cdots YZ}_{DE}\right)}\frac{(p-2)!P^k_{(p-2)f\cdots yzw}}{\mathbb{R}^1_{f\cdots yz}!\mathbb{R}^2_{f\cdots yz}!\cdots\mathbb{R}^{\gamma}_{f\cdots yz}!}\\
-&\frac{2!\lambda^k_{(2)df}}{\mathbb{R}^1_{df}!\left(1+\tau^{E\cdots MN}_{DF}\right)}\frac{(p-2)!P^k_{(p-2)e\cdots mnw}}{\mathbb{R}^1_{e\cdots mn}!\mathbb{R}^2_{e\cdots mn}!\cdots\mathbb{R}^{\eta}_{e\cdots mn}!}-\cdots-\frac{2!\lambda^k_{(2)DN}}{\mathbb{R}^1_{dn}!\left(1+\tau^{E\cdots LM}_{DN}\right)}\frac{(p-2)!P^k_{(p-2)E\cdots LMw}}{\mathbb{R}^1_{e\cdots lm}!\mathbb{R}^2_{e\cdots lm}!\cdots\mathbb{R}^{\kappa}_{e\cdots lm}!}\\
-&\frac{2!\lambda^k_{(2)EF}}{\mathbb{R}^1_{ef}!\left(1+\tau^{D\cdots MN}_{EF}\right)}\frac{(p-2)!P^k_{(p-2)d\cdots mnw}}{\mathbb{R}^{\phi 1}_{d\cdots mn}!\mathbb{R}^{\phi 2}_{d\cdots mn}!\cdots\mathbb{R}^{\mu}_{d\cdots mn}!}-\cdots-\frac{2!\lambda^k_{(2)EN}}{\mathbb{R}^1_{en}!\left(1+\tau^{D\cdots LM}_{EN}\right)}\frac{(p-2)!P^k_{(p-2)D\cdots LMw}}{\mathbb{R}^1_{d\cdots lm}!\mathbb{R}^2_{d\cdots lm}!\cdots\mathbb{R}^{\nu}_{d\cdots lm}!}\\
-\cdots-&\frac{2!\lambda^k_{(2)MN}}{\mathbb{R}^1_{mn}!\left(1+\tau^{DE\cdots L}_{MN}\right)}\frac{(p-2)!P^k_{(p-2)DE\cdots Lw}}{\mathbb{R}^1_{de\cdots l}!\mathbb{R}^2_{de\cdots l}!\cdots\mathbb{R}^{\varpi}_{de\cdots l}!}\\
-\cdots-&\frac{(p-1)!\lambda^k_{(p-1)EF\cdots N}}{\mathbb{R}^1_{ef\cdots n}!\mathbb{R}^2_{ef\cdots n}!\cdots\mathbb{R}^{\beta}_{ef\cdots n}!\left(1+\tau^{d}_{EF\cdots N}\right)}P^k_{(1)dw}-\frac{(p-1)!\lambda^k_{(p-1)DF\cdots N}}{\mathbb{R}^1_{df\cdots n}!\mathbb{R}^2_{df\cdots n}!\cdots\mathbb{R}^{\chi}_{df\cdots n}!\left(1+\tau^{e}_{DF\cdots N}\right)}P^k_{(1)ew}\\
-\cdots-&\frac{(p-1)!\lambda^k_{(p-1)DE\cdots M}}{\mathbb{R}^1_{de\cdots m}!\mathbb{R}^2_{de\cdots m}!\cdots\mathbb{R}^{\varphi}_{de\cdots m}!\left(1+\tau^{z}_{DE\cdots M}\right)}P^k_{(1)nw}\Bigg]
\end{aligned}
\tag{31}
$$

All these eigenvalue and eigenvector coefficients can be computed using a perturbation algorithm described as follows. With the known changes of the eigenvalues, $\lambda^k_d-\lambda^k$, in Eq. 4 and those of the eigenvectors, $\overline{\phi}^k_d-\overline{\phi}^k$, in Eq. 5, the perturbation equations at each estimation are generated. The changes of all stiffness parameters are then calculated from these equations using DFP Quasi-Newton optimization method.

3 Computational aspect of the perturbation algorithm

The objective in the perturbation algorithm is to estimate the stiffness parameters of the structure so that its eigenparameters from the computational model closely resemble those from the damaged case, $\overline{\Phi}_D = \left(\lambda_D^1, \overline{\phi}_D^1, \lambda_D^2, \overline{\phi}_D^2, \ldots, \lambda_D^n, \overline{\phi}_D^n\right)^T$. The algorithm reads in and transforms the eigenparameter of the original computational structure to its master degrees of freedom (d.o.f.s). Impaction of the work lies on the use of elastic modulus as monitoring parameter, for which not just Young's modulus can be changed but also its physical dimensions, such as width and thickness. This availability is essential in the corrosion detection of lightning pole in an electrical substation in Baltimore city of Maryland [21], where cross-sectional area of the lightning pole reduced in significant proportion after a long period of outdoor services. Our ultimate goal is to estimate the elastic moduli, $G_d = E_d I / l_e^3$ (where E_d is the Young's modulus of the d-th element, I and l_e are its moment of inertia and length, respectively), of the structural components which serve as the structural parameters of the system. With the use of explicit perturbation coefficient equations, these coefficients can be constructed progressively from the lower-order terms. From the developed methodology the left-hand sides of the system equations, such as Eqs. 4 and 5, are $\overline{\phi}_D^k$ and λ_D^k from the simulated data of the damaged case, and the first terms on the right-hand sides of these equations are the eigenparameters of the computational model from previous estimation. In the first estimation, λ^k and $\overline{\phi}^k$ in the system equations are the updated eigenparameters of the undamaged beam. Substituting these coefficients in Eqs. 4 and 5, the system perturbation equations are formed. The changes to the elastic moduli are optimized using DFP Quasi-Newton method [22]. We use the notations, ε_λ^k and $\overline{\varepsilon}_\phi^k$, to denote errors in satisfying the system equations Eqs. 4 and 5 respectively. We choose a set of n eigenparameter pairs in the detection process. Let the number of master d.o.f.s of $\overline{\phi}_d^k$ be N_m, $N_m = N$ and $N_m < N$ when we have complete and reduced order eigenvector measurements, respectively. Hence we establish the weighted eigenparameter perturbation residual objective function as

$$J = \sum_{k=1}^{n} W_\lambda^k \left(\varepsilon_\lambda^{k(p)}\right)^2 + \sum_{k=1}^{n} W_{\overline{\phi}}^k \left(\overline{\varepsilon}_\phi^{k(p)}\right)^T \left(\overline{\varepsilon}_\phi^{k(p)}\right) \tag{32}$$

where $W_\lambda^k (k = 1, 2, \ldots, n)$ and $W_{\overline{\phi}}^k (k = 1, 2, \ldots, n)$ are the weighting factors, and J is a function of $\delta G_d^{(w)}$ when one substitutes the expressions for $\varepsilon_\lambda^{k(p)}$ and $\overline{\varepsilon}_\phi^{k(p)}$ in Eqs. 4–5 into Eq. 32. This is an over-determined system, where $n + nN_m > m$, and the DFP Quasi-Newton approach is used to determine $\delta G_i^{(w)}$ iteratively. Meanwhile, $J = 0$ (i.e. $\varepsilon_\lambda^{k(p)} = \overline{\varepsilon}_\phi^{k(p)} = 0$) when the optimal solutions are reached. To minimize the objective function in Eq. 32 at the w-th iteration, one can use the Quasi-Newton optimization approach

$$\delta \overline{G}_{(b)}^{(w)} = \delta \overline{G}_{(b-1)}^{(w)} - \alpha_b B_{b-1} \overline{g}_{b-1} \tag{33}$$

to update the variations in the stiffness parameters, where $\delta \overline{G}_{(b)}^{(w)} = \left(\delta G_{1(b)}^{(w)}, \delta G_{2(b)}^{(w)}, \ldots, \delta G_{m(b)}^{(w)}\right)^T$, $\alpha_b \geq 0$ is the step size, and the gradient vector associated with $\delta \overline{G}_{(b-1)}^{(w)}$ equals $\overline{g}_{b-1} = \left(\frac{\partial J}{\partial G_1^{(w)}}, \frac{\partial J}{\partial G_2^{(w)}}, \ldots, \frac{\partial J}{\partial G_m^{(w)}}\right)^T$. Note that the subscript b ($b \geq 1$) in all variables in Eq. 33 denotes the number of nested iterations. The initial values used are $\delta G_{d(0)}^{(w)} = 0$. The nested iteration is terminated when $\alpha_b \left\|\overline{g}_{b-1}\right\|_\infty < \gamma$, where $\|\cdot\|_\infty$ is the infinity norm and γ is some small constant, or the number of nested iterations exceeds an acceptable number, D.

Due to its successive linear approximations to the objective function, the gradient algorithm may progress slowly when approaching a stationary point. DFP Quasi-Newton method provides a remedy to this problem by using essentially quadratic approximation to the objective function near the stationary point. Its iteration scheme is given by Eq. 33, where B_{b-1} is an approximation to the inverse of the Hessian matrix used at the b-th nested iteration. Initially, we set $\delta G_{d(0)}^{(w)} = 0$ and $B_0 = I$ as the identity matrix. The matrix B_b is updated using the DFP formula

$$B_b = B_{b-1} + \frac{\left(\delta \overline{G}_{(b)}^{(w)} - \delta \overline{G}_{(b-1)}^{(w)}\right)\left(\delta \overline{G}_{(b)}^{(w)} - \delta \overline{G}_{(b-1)}^{(w)}\right)^T}{\left(\delta \overline{G}_{(b)}^{(w)} - \delta \overline{G}_{(b-1)}^{(w)}\right)^T \left(\overline{g}_b - \overline{g}_{b-1}\right)} - \frac{\left[B_{b-1}\left(\overline{g}_b - \overline{g}_{b-1}\right)\right]\left[B_{b-1}\left(\overline{g}_b - \overline{g}_{b-1}\right)\right]^T}{\left(\overline{g}_b - \overline{g}_{b-1}\right)^T B_{b-1}\left(\overline{g}_b - \overline{g}_{b-1}\right)} \tag{34}$$

The nested iteration is terminated when $\alpha_b \left\| B_{b-1}\overline{g}_{b-1} \right\|_\infty < \gamma$ or the number of iterations exceeds D. The optimization process, including the step size search procedure, is described below. When the b nested iteration is completed, elastic moduli in this computational model are then updated by

$$G_d^{(w+1)} = G_d^{(w)} + \delta G_d^{(w)}. \tag{35}$$

where $\delta G_d^{(w)}$ is the estimated change of the d-th elastic modulus. Note that in each subsequent estimation (i.e., $w \geq 2$), Eqs. 4 and 5 are modified by replacing elastic moduli $G_d, G_e, \ldots,$ and G_z with $G_d^{(w)}, G_e^{(w)}, \ldots,$ and $G_z^{(w)}$, respectively while all the selected eigenparameters and their coefficients are reanalyzed using the modular beam model. From the calculated changes of the eigenparameters on the left-hand sides of the resulting perturbation equations, one calculates inversely the change of the elastic modulus $\delta G_d^{(w)}$ and updates the elastic modulus using Eq. 33. Two process indicators are used during the estimation process:

(1) Process criterion is attained when the total norm of the weighted normalized eigenparameter difference vector drops below $dn\%$ of the normalized eigenparameter difference vector (d-norm)

$$\begin{aligned} \|d\|^{(w_{dn})} &= n_{\overline{\phi}_d} \sum_{i=1}^{n_\phi} W_{\overline{\phi}_d^i} \left\| \frac{\overline{\phi}^{i(w_{dn})} - \overline{\phi}_d^i}{\max\left|\overline{\phi}_d^i\right|} \right\| + \sum_{j=1}^{n_\lambda} W_{\lambda_d^j} \left\| \frac{\lambda^{j(w_{dn})} - \lambda_d^j}{\lambda_d^j} \right\| \\ &\leq \frac{dn}{100} \left(n_{\overline{\phi}_d} \sum_{i=1}^{n_\phi} W_{\overline{\phi}_d^i} \left\| \frac{\overline{\phi}^{i(0)} - \overline{\phi}_d^i}{\max\left|\overline{\phi}_d^i\right|} \right\| + \sum_{j=1}^{n_\lambda} W_{\lambda_d^j} \left\| \frac{\lambda^{j(0)} - \lambda_d^j}{\lambda_d^j} \right\| \right) \end{aligned} \tag{36}$$

where $n_{\overline{\phi}_d^i}$ is the total d.o.f.s of $\overline{\phi}_d^i$, $W_{\overline{\phi}_d^i}$ is the weighting factor of the i-th damaged eigenvector, $W_{\lambda_d^j}$ is the weighting factor of the j-th damaged eigenvalue, w_{dn} is the smallest estimation number for which the dn % termination criterion is reached.

(2) Termination criterion is attained when the norm of the normalized eigenparameter difference vector drops below $tn\%$ of the total norm of weighted normalized damaged eigenparameter vector (t-norm)

$$\begin{aligned} \|d\|^{(w_{tn})} &= n_{\overline{\phi}_d} \sum_{i=1}^{n_{\overline{\phi}}} W_{\overline{\phi}_d^i} \left\| \frac{\overline{\phi}^{i(w_{tn})} - \overline{\phi}_d^i}{\max\left|\overline{\phi}_d^i\right|} \right\| + \sum_{j=1}^{n_\lambda} W_{\lambda_d^j} \left\| \frac{\lambda^{j(w_{tn})} - \lambda_d^j}{\lambda_d^j} \right\| \\ &\leq \frac{tn}{100} \left(n_{\overline{\phi}_d} \sum_{i=1}^{n_{\overline{\phi}}} W_{\overline{\phi}_d^i} \left\| \frac{\overline{\phi}_d^i}{\max\left|\overline{\phi}_d^i\right|} \right\| + \sum_{j=1}^{n_\lambda} W_{\lambda_d^j} \right) \end{aligned} \tag{37}$$

where w_{tn} is the smallest estimation number for which the tn % termination criterion is reached. From Eqs. 36 and 37, one can note that these process indicators are dimensionless numbers. In order to automate the whole process, the algorithm is established under the MatLab programming platform. It integrates the modular beam's finite element model, vibration analysis, explicit coefficient generation, perturbation equation establishment and optimization solver. Its main steps are listed below:

(1) Construct the system matrices of the eigenvalue equation for the modular beam.
(2) Compute the eigenparameters of the damaged and updated modular beam.
(3) Calculate the explicit eigenvalue and eigenvector perturbation coefficients
(4) Set up the inverse system perturbation equations.
(5) Estimate $\delta\overline{G}^{(w)}$ from perturbation equations using Quasi-Newton method.
(6) Update the stiffness parameter vector.
(7) Repeat step (1) to (6) iteratively until both process indicators are attained.
(8) Plot out the estimation curves of the beam's elastic moduli.

4 Structural damage detection of modular beam

After developing the algorithm, its performance was evaluated through different damaged cases. Random damages are applied to all beam elements with systematic range (i.e. at the same range) from small, medium to large damage percentages. This type of damage occurs when the beams damage progressively under the external environmental loads, such as erosion, lightning, thermal creep or wind gust. This type of load is applied externally to all surfaces of the structure giving rise to the systematic rusting, corrosion or stiffness reduction.

4.1 Computational model of modular beam

To investigate the applicability on different orders of the developed algorithm, various damaged cases are introduced to a modular beam model which has been applied to damage detection of lightning poles in the Texas electrical substation of Baltimore Gas and Electric Corporation [21]. The beam has the length $L_t = 0.7$ m, width $W = 0.0254$ m, thickness $H = 0.0031$ m, area moment of inertia $I = WH^3/12 = 6.3058 \times 10^{-11}\text{m}^4$ and mass density $\rho = 2715\text{kg/m}^3$and healthy Young's modulus $E_h = 6.9 \times 10^{10}\text{N/m}^2$. Its finite element model shown in Fig. 1 is used to model its planar transverse vibrations. The beam is divided into $N_e = m$ elements with length of each element being $l_e = L_t/N_e$, and there are $N_e + 1$ nodes. With V_d and θ_d denoting the y-translational and rotational displacements at d-th node ($d = 1, 2, \ldots, N_e + 1$), the nodal displacement vector of the d-th element is $\overline{q}_d^e = \left[V_d, \theta_d, V_{d+1}, \theta_{d+1}\right]^T$. Under bending force F^y and moment M^z, the nodal force vector is $\overline{F}_d^e = \left[F_d^y, M_d^z, F_{d+1}^y, M_{d+1}^z\right]^T$.

At first, direct stiffness method [15] is utilized to formulate the element mass matrix. For small elastic deformation, these two vectors are connected by the linear element stiffness equation

$$\overline{F}_d^e = K_d^e \overline{q}_d^e \tag{38}$$

where

$$K_d^e = \begin{bmatrix} k_{11} & k_{12} & k_{13} & k_{14} \\ k_{21} & k_{22} & k_{23} & k_{24} \\ k_{31} & k_{32} & k_{33} & k_{34} \\ k_{41} & k_{42} & k_{43} & k_{44} \end{bmatrix}$$

is the d-th element stiffness matrix. Making use of force and moment balance, setting $V_d = 1$ while keeping other displacements equal zero at d-th node, we have

$$\begin{aligned} V_d &= \frac{F_d^y l_e^3}{3E_d I} - \frac{M_d^z l_e^2}{2E_d I} = 1 \\ \theta_d &= -\frac{F_d^y l_e^2}{2E_d I} + \frac{M_d^z l_e}{E_d I} = 0 \end{aligned} \tag{39}$$

From this equation set, one can get $F_d^y = 12E_d I/l_e^3$ and $M_d^z = 6E_d I/l_e^2$. From the static equilibrium condition, $F_{d+1}^y = -F_d^y = -12E_d I/l_e^3$, $M_{d+1}^z = F_d^y l_e - M_d^z = 6E_d I/l_e^2$. Substituting these terms into

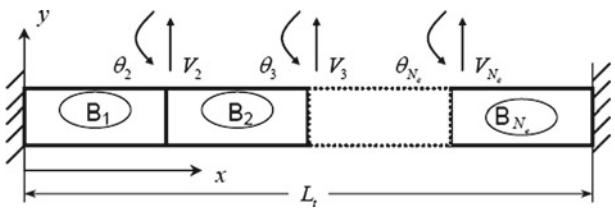

Fig. 1 Computational model of modular beam with fixed–fixed boundary conditions

Eq. 38, it can solve $k_{11} = F_d^y = 12E_dI/l_e^3, k_{21} = M_d^z = 6E_dI/l_e^2, k_{31} = F_{d+1}^y = -12E_dI/l_e^3$ and $k_{41} = M_{d+1}^y = 6E_dI/l_e^2$. Now setting $\theta_d = 1$ and other displacements to zero,

$$\begin{aligned} V_d &= \frac{F_d^y l_e^3}{3E_dI} - \frac{M_d^z l_e^2}{2E_dI} = 0 \\ \theta_d &= -\frac{F_d^y l_e^2}{2E_dI} + \frac{M_d^z l_e}{E_dI} = 1 \end{aligned} \tag{40}$$

This equation set gives $F_d^y = 6E_dI/l_e^2$ and $M_d^z = 4E_dI/l_e$. According to static equilibrium condition, $F_{d+1}^y = -F_d^y = -6E_dI/l_e^2, M_{d+1}^z = F_d^y l_e - M_d^z = 2E_dI/l_e$. Solving Eq. 38, one can obtain $k_{12} = F_d^y = 6E_dI/l_e^2, k_{22} = M_d^z = 4E_dI/l_e, k_{32} = F_{d+1}^y = -6E_dI/l_e^2$ and $k_{42} = M_{d+1}^z = 2E_dI/l_e$. Similarly, by setting unity on the displacements at d+1-th node, we can finalize the d-th element stiffness matrix as

$$K_d^e = \frac{E_dWH^3}{12l_e^3}\begin{bmatrix} 12 & 6l_e & -12 & 6l_e \\ 6l_e & 4l_e^2 & -6l_e & 2l_e^2 \\ -12 & -6l_e & 12 & -6l_e \\ 6l_e & 2l_e^2 & -6l_e & 4l_e^2 \end{bmatrix} \tag{41}$$

Utilizing this matrix, one can extract out the term $G_d = E_dWH^3/12l_e^3$, which is the elastic modulus of the beam element. Its value in healthy six elements beam is $G_h = 2.74 \times 10^3$ N/m. Moreover, this term validated the assumption that the stiffness matrix is first order with respect to G_d as discussed in Eq. 3. Small, medium and large percentage damages, which correspond to the reduction in elastic moduli of 0–30, 30–60 and 60–90%, respectively, are simulated on the beam.

At second, virtue work principle is utilized to formulate the element stiffness matrix. Without loss of generality, y-translational displacement is represented by cubic Hermite curve with respect to x [15],

$$V_x = \alpha_1 + \alpha_2 x + \alpha_3 x^2 + \alpha_4 x^3 \tag{42}$$

And rotational displacement $\theta_x$is the derivative of V_x given by

$$\theta_x = \alpha_2 x + 2\alpha_3 x + 3\alpha_4 x^2 \tag{43}$$

Eqs. 42–43 can be represented in matrix form

$$\begin{Bmatrix} V_x \\ \theta_x \end{Bmatrix} = \begin{bmatrix} 1 & x & x^2 & x^3 \\ 0 & 1 & 2x & 3x^2 \end{bmatrix} \begin{Bmatrix} \alpha_1 & \alpha_2 & \alpha_3 & \alpha_4 \end{Bmatrix}^T = \begin{bmatrix} S_V \\ S_\theta \end{bmatrix} \overline{\alpha}^e = S\overline{\alpha}^e \tag{44}$$

This is the displacement equation of any point within the element. From this relation, one can obtain the start and end point equations at $x = 0, l_e$, respectively:

$$\begin{Bmatrix} V_d \\ \theta_d \\ V_{d+1} \\ \theta_{d+1} \end{Bmatrix} = \begin{bmatrix} 1 & 0 & 0 & 0 \\ 0 & 1 & 0 & 0 \\ 1 & l_e & l_e^2 & l_e^3 \\ 0 & 1 & 2l_e & 3l_e^2 \end{bmatrix} \{ \alpha_1 \quad \alpha_2 \quad \alpha_3 \quad \alpha_4 \}^T = A \{\alpha\} \tag{45}$$

where A is the displacement matrix of end points. Using its inverse, the shape function vector is obtained as

$$\overline{N}_e = S_V A^{-1} = \frac{1}{l_e^3}\left\{ l_e^3 - 3x^2 l_e^+ 2x^3 \quad x l_e^3 - 2x^2 l_e^2 + x^3 l_e \quad 3x^2 l_e - 2x^3 \quad -x^2 l_e^2 + x^3 l_e \right\} \tag{46}$$

By the virtue work principle, the element mass matrix is obtained by substituting $\overline{N}_e$ as

$$M_d^e = \int_0^{l_e} \rho WH \overline{N}_e^T \overline{N}_e^d x = \frac{\rho WHl_e}{420}\begin{bmatrix} 156 & 22l_e & 54 & -13l_e \\ 22l_e & 4l_e^2 & 13l_e & -3l_e^2 \\ 54 & 13l_e & 156 & -22l_e \\ -13l_e & -3l_e^2 & -22l_e & 4l_e^2 \end{bmatrix} \tag{47}$$

Table 1 Eigenvalue errors of undamaged finite element beam when compared with Euler–Bernoulli beam

Mode	E–B Beam	6 Elements	% Error	8 Elements	% Error	10 Elements	% Error
1	14.34	14.31	0.2	14.34	−0.01	14.35	−0.06
2	23.81	23.6	0.88	23.73	0.3	23.79	0.07
3	33.33	33.07	0.8	33.11	0.67	33.23	0.32
4	42.86	43.24	−0.88	42.62	0.57	42.64	0.5
5	52.38	53.86	−2.75	52.52	−0.26	52.17	0.41

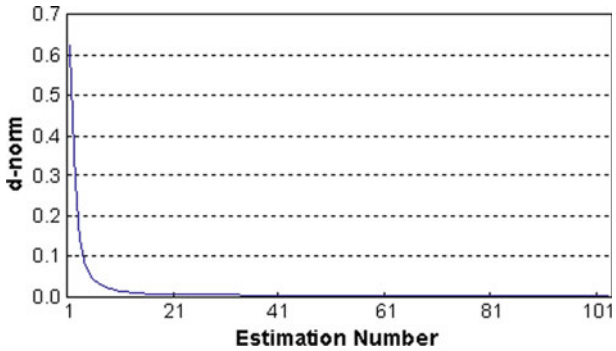

Fig. 2 Case 6o1_rs: d-norm of six elements beam using first-order algorithm (0.7–$1.0G_h$)

For this analysis, the mass matrix is kept constant among different elements. As l_e is constant inside the matrix, the term $\rho W H l_e/420$ is constrained to be constant. Using the standard assembly process yields the system mass matrix of Eq. 1, i.e.$M = \sum_{d=1}^{N_e} M_d^e$. For the initial element at $d = 1$, the 4×4 element mass matrix of Eq. 47 is assembled to the system mass matrix at d.o.f.s 1 to 4. At intermediate element ($d = i$), the element mass matrix is assembled to the system mass matrix at d.o.f.s $2i - 1$to $2i + 2$. For the final element at $d = N_e$, the element mass matrix is assembled to the d.o.f.s $2N_e - 1$ and $2N_e + 2$. Similarly, system stiffness matrix is assembled as $K = \sum_{d=1}^{N_e} K_d^e$ where its dimensions are $2(N_e+1) \times 2(N_e+1)$. Now we should set the boundary conditions for this fixed–fixed beam. By constraining the translational and rotational displacements, d.o.f.s 1 and 2 are eliminated at the first node while d.o.f.s $2N_e + 1$ and $2N_e + 2$ are eliminated at the $(N_e + 1)$-th node. Thus, the M and K matrices are generated with dimensions $2\,(N_e - 1) \times 2\,(N_e - 1)$, where $2\,(N_e - 1)$ is the d.o.f.s of the system. Displacement vector of the system containing the unconstrained nodes becomes the eigenvector $\overline{\phi}^k = [V_2, \theta_2, V_3, \theta_3, \ldots, V_{N_e}, \theta_{N_e}]^T$, which is obtained by solving the eigenvalue equation in Eq. 1 or 2. For checking the accuracy of the finite element approach of beam model, its undamaged eigenvalues are compared with the closed-form Euler–Bernoulli (E–B) beam in Table 1. From the table, one can notice that in six elements beam, there is scattering of discretization errors among five eigenvalues with the largest deviation in fifth mode. This is explained by the curvature order error in the cubic Hermite curve. This error increases drastically when the curvature order of E–B beam is higher than that of the Hermite function. As a result, the percentage error in the fifth mode is extra high. On the other hand, the order of curvature in each element decreases with the increasing number of elements. Thus, the effect of curvature mismatch is lessened. Overall, discretization errors decrease with the increase in the element number. When the number of nodal point increases, the estimated eigenparameters are more close to that of the infinite E–B beam. In order to evaluate the performances of different order algorithms, various levels of random damages are introduced to this modular beam with six to ten number of elements from cases 6o1_rs to 10o2_rs to establish its systematic random damage cases.

4.2 Small percentage systematic damage

At first, first-order algorithm is developed by the perturbation equations Eqs. 4 and 5 with terms up to δG_d. Using this algorithm in case 6o1_rs for the small percentage damages $0.7G_h \leq G_d \leq 1.0\,G_h$ with $N_e = 6$, $W_{\overline{\phi}_d^i} = 1$, $W_{\lambda_d^j} = 0.2$, $dn = 1$ and $tn = 10^{-4}$. The d-norm drops rapidly from 6.24×10^{-1} to its process criterion at 5.37×10^{-3} in 21 estimations in a curved region (Fig. 2). Afterward, it remains at a flat plateau

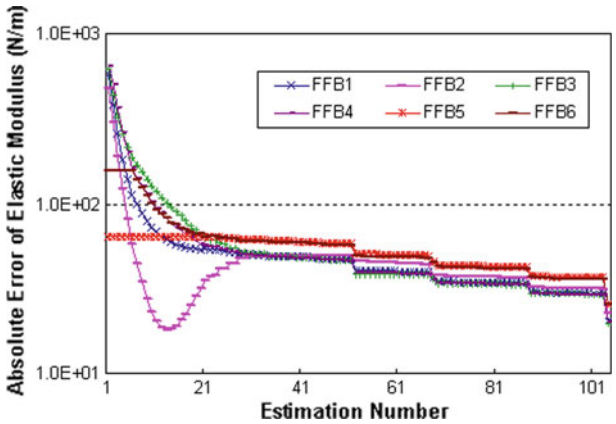

Fig. 3 Case 6o1_rs: logarithmic absolute errors of six elements beam using first-order algorithm (0.7–1.0G_h)

Table 2 Convergence numbers of six elements beam damage detection

Case	Process criterion	Termination criterion
6ol_rs	21	104
6o2_rs	21	112
6ol_rm	9	57
6o2_rm	9	42
6ol_rl	19	>200
6o2 rl	33	146

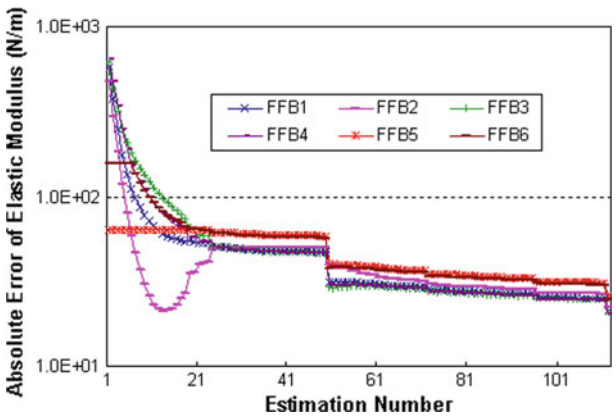

Fig. 4 Case 6o2_rs: logarithmic absolute errors of six elements beam using second-order algorithm (0.7–1.0G_h)

until 10^{-4} t-norm termination criterion is reached. From its logarithmic absolute error chart of Fig. 3, one can observe that elements FFB1 to 4 drop rapidly and gradually toward the first cliff region. Element FFB6 remains at 157 N/m level until estimation 6, then it drops gradually. Element FFB6 is limited by the first cliff level. Then, they drop stepwise at estimation 52 in the first cliff region. Afterward, they drop stepwise regularly reaching t-norm criterion at estimation 104 as listed in Table 2.

Meanwhile, utilizing Eqs. 4 and 5 with terms up to $\delta G_d \delta G_e$, second-order algorithm is developed. By this algorithm in case 6o2_rs, its convergence is shown in Table 2. The d-norm drops rapidly from 6.24×10^{-1} to 6.00×10^{-3} in 21 estimations where d-norm criterion is reached. Afterward, it remains at a flat plateau until t-norm criterion is reached. From the logarithmic absolute error chart of Fig. 4, one can observe that the elements converge in a very similar convergence pattern as those of case 6o1_rs. The t-norm criterion is attained at estimation 112. Therefore, the second-order terms have slightly delayed the convergence in small percentage damage range.

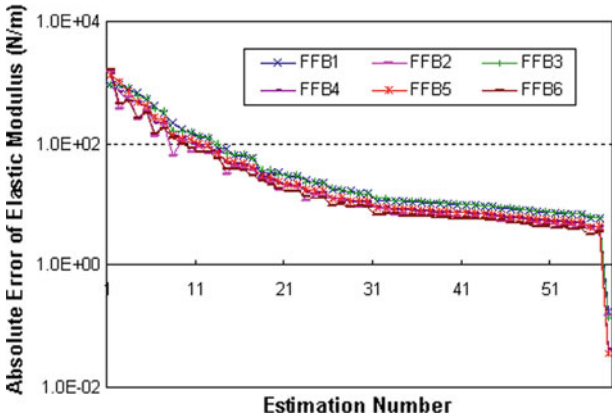

Fig. 5 Case 6o1_rm: logarithmic absolute errors of six elements beam using first-order algorithm (0.4–0.7G_h)

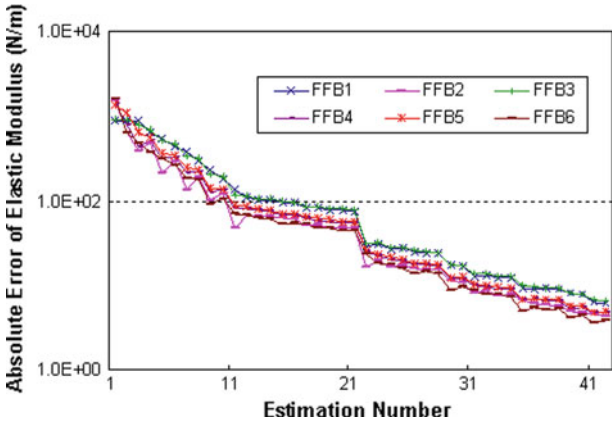

Fig. 6 Case 6o2_rm: logarithmic absolute errors of six elements beam using second-order algorithm (0.4–0.7G_h)

4.3 Medium percentage systematic damage

At second, using the first-order algorithm of case 6o1_rm in detecting medium percentage damages, $0.4G_h \leq G_d \leq 0.7G_h$, the d-norm drops to its process criterion rapidly from 9.04 to 8.20×10^{-2} at estimation 9. Then it drops continuously and gradually to t-norm criterion until estimation 57. From the logarithmic absolute error chart in Fig. 5, one can observe that elements FFB2, 4 to 6 interact vigorously until estimation 11. Meanwhile, elements FFB1 and 3 are limited around 900 level at the first two estimations. Afterward, they propagate until the t-norm criterion is attained. All elements propagate in straight lines with the same slope between estimations 31 to 56. Therefore, they are converging exponentially in this region. For the second-order algorithm in case 6o2_rm, the d-norm drops to its criterion rapidly from 1.43 to 1.24×10^{-2} at estimation 9. Then it drops gradually to t-norm criterion. The logarithmic absolute error chart in Fig. 6 indicates very similar convergence patterns as case 6o1_rm, except that the t-norm criterion is attained at estimation 42 (Table 2). The second-order terms contribute slight significantly in medium percentage damage range.

4.4 Large percentage systematic damage

At third, first-order algorithm of case 6o1_rl is applied to the large percentage random damages ($0.1G_h \leq G_d \leq 0.4G_h$) with the d-norm chart. The d-norm drops to its criterion vigorously from 152 to 1.08 at estimation 19. Then it converges gradually toward the t-norm, but is not attained before the maximum number of estimation 200. From the logarithmic absolute error chart at Fig. 7, one can observe that element FFB6 is limited at 1.75×10^3 level until estimation 7. Other elements interact chaotically until estimation 18. Then they all converge gradually toward the ultimate solution. For the second-order algorithm of case 6o2_rl, d-norm drops to its criterion vigorously from 18.1 to 1.75×10^{-1} at estimation 33. Then it converges gradually toward

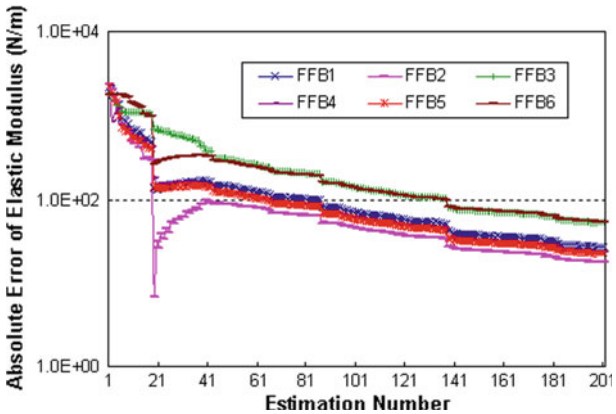

Fig. 7 Case 6o1_rl: logarithmic absolute errors of six elements beam using first-order algorithm (0.1–0.4G_h)

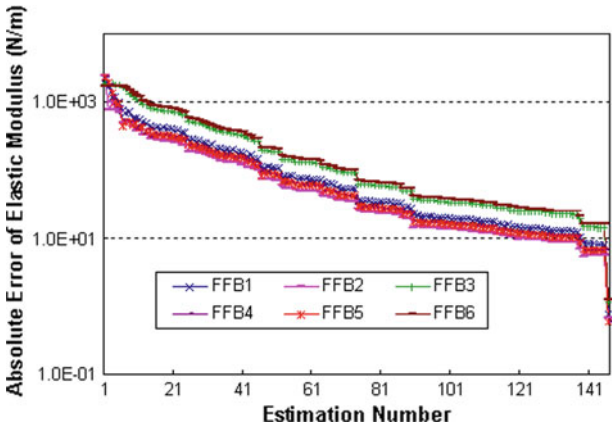

Fig. 8 Case 6o2_rl: logarithmic absolute errors of six elements beam using second-order algorithm (0.1–0.4G_h)

the t-norm criterion. The logarithmic absolute error chart at Fig. 8 indicates that element FFB6 is limited at 1.75×10^3 level until estimation 5. Other elements interact chaotically until estimation 7. Then they all converge gradually toward the t-norm criterion at estimation 146 as in Table 2. The elements propagate in straight lines with the same slope between estimations 91 and 138. Therefore, they are converging with same exponential rate in this region. Thus, the second-order terms have significant contribution in large percentage damage range.

In summary, under the 1% d-norm process criterion, the convergence of both algorithms is the same for small and medium percentage damages. And for large percentage damages, first-order algorithm is more efficient than the second-order algorithm. Moreover, under the 10^{-4} t-norm termination criterion, the convergence of first-order algorithm is slightly more effective for small percentage damages. In medium percentage damages, the second-order algorithm is more effective. Meanwhile for large percentage damages, first-order algorithm does not converge while the second-order algorithm converges effectively.

4.5 Damage detection of eight and ten elements beam

As revealed from Table 3, for the eight elements large percentage damages with $N_e = 8$, second-order algorithm (estimation 14) converges faster than first-order algorithm (estimation 25) under d-norm criterion. Also for the t-norm criterion, second-order algorithm (estimation 54) converges faster than first-order algorithm (estimation 87). One can observe from its logarithmic absolute error chart (Fig. 9) that element FFB1 propagates in a zigzag pattern while other elements propagate in line patterns with constant slopes. Exponential convergences are observed for all elements when their sequence magnitudes are established. So they can converge directly to the t-norm criterion in fewer estimations by relaxing the constraints at the perturbation

Table 3 Convergence numbers of eight and ten elements beam damage detection

Case	Process criterion	Termination criterion
8ol_rl	14	87
8o2_rl	25	54
l0ol_rs	48	181
10o2_rs	37	55

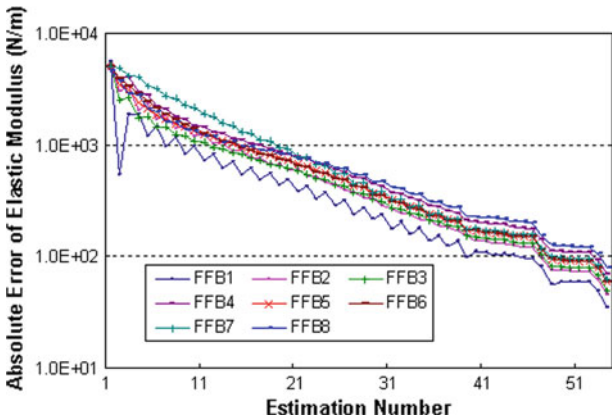

Fig. 9 Case 8o2_rl: logarithmic absolute errors of eight elements beam using second-order algorithm (0.1–0.4G_h)

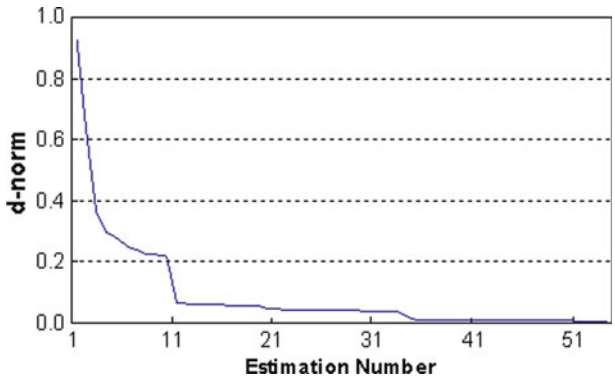

Fig. 10 Case 10o2_rs: d-norm of ten elements beam using second-order algorithm (0.7–1.0G_h)

ranges. Besides, there should be some definite relationships between the convergences and the perturbation algorithms which need to be further investigated.

Now for the ten elements small percentage damages with $N_e = 10$, the first-order algorithm converges slower to the d-norm criterion. Meanwhile in the t-norm criterion, second-order algorithm (estimation 55) converges much faster than first-order algorithm (estimation 181). Using the d-norm chart in Fig. 10, the d-norm drops rapidly then propagates gradually toward the first cliff at estimation 10. Then it drops and propagates in the plateau region. Afterward it drops at the second cliff on estimation 34, reaching the second plateau region where the d-norm process criterion is satisfied at estimation 37. Ultimately, it converges to the t-norm criterion at estimation 55 where less than 0.1% d-norm is attained. From Fig. 11 the convergence pattern is separated into several regions. In the first region, all elements oscillate with different patterns until the first cliff at estimation 10. Then they drop stepwise one by one in the plateau region, where the second cliff is located at estimation 33. And for the third region, they propagate steadily in the plateau until the third cliff at estimation 54. Afterward, they remain stable toward the t-norm termination criterion.

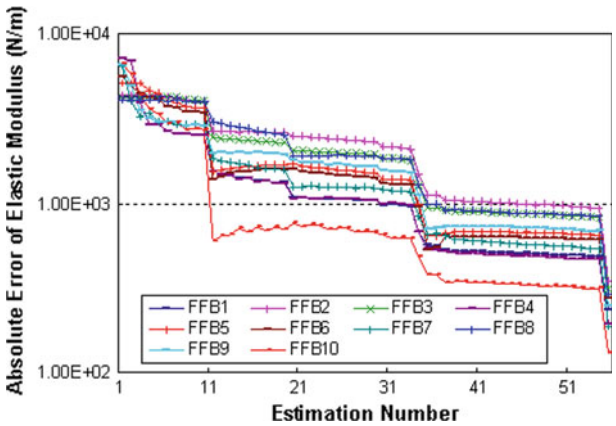

Fig. 11 Case 10o2_rs: logarithmic absolute errors of ten elements beam using second-order algorithm (0.7–1.0G_h)

5 Conclusion

Using the perturbation theory, the structural damage detection problem was formulated by solving the perturbation equations inversely. At first, by introducing the specific permutation numbers and generalized Kronecker delta, the explicit generalized-order perturbation coefficients were derived rigorously. Initially, the skew-symmetric properties of these eigenparameter coefficients were preserved. Then, the symmetric eigenparameter coefficients were obtained by factorial numbers. At second, these equations were solved by the DFP Quasi-Newton optimization solver. Automated algorithm for a modular beam was programmed. Finite element formulation of the beam is derived from the direct stiffness and virtue work principles of plane beam structure. When compared with the E–B beam, curvature errors increase drastically when the order of E–B beam curvature is higher than that of the Hermite curve. Discretization errors decrease with the increase in the element number as it approaches the infinite beam.

Damage detection process is carried out using logarithmic absolute error chart. In the six elements beam, the significance of second-order terms increases as the percentage of the damages increases. This adequately demonstrated that the generalized-order terms are essential for improving the convergent rate toward large percentage cases. Moreover, for eight elements beam with large percentage damage, first-order algorithm converges faster in the 1% d-norm, while it is faster for the second-order algorithm in the 10^{-4}% t-norm. Furthermore, for ten elements beam with small percentage damage, second-order algorithm converges faster in the d-norm criterion and much faster in the t-norm criterion. Exponential patterns are observed in logarithmic absolute error charts of several cases, which may enhance the convergences. Their relationships with the perturbation algorithms require further investigations.

Acknowledgments The authors greatly appreciate the grants from the Jinchuan Group Ltd. under the contract number H04010801W080421, and the Research Initiative Fund of School of Mechatronic Engineering in the UESTC. In addition, the authors gratefully thank Dr. K.T. Chan of The Hong Kong Polytechnic University for the vibration model of this work.

References

1. Rayleigh, B.: The theory of sound, vol. 1, pp. 214–217. Dover, New York (1945)
2. Wilkenson, J.H.: The algebraic eigenvalue problem. Clarendon Press, Oxford (1965)
3. Bellman, R.: Introduction to matrix analysis, pp. 60–63, 2nd edn. McGraw-Hill Book Co, New York (1970)
4. Romstad, K.M., Hutchinson, J.R., Runge, K.H.: Design parameter variation and structural response. Int. J. Num. Methods Eng. **5**, 337–349 (1973)
5. Stetson, K.A.: Perturbation method of structural design relevant to holographic vibration analysis. AIAA J. **13**, 457–459 (1975)
6. Meirovitch, L., Ryland, G.: A perturbation technique for gyroscopic systems with small internal and external damping. J. Sound Vib. **100**(3), 393–408 (1985)
7. Meirovitch, L., Ryland, G.: Response of lightly damped gyroscopic systems. J. Sound Vib. **67**, 1–19 (1979)
8. Jones, R.P.N.: The effect of small changes in mass and stiffness on the natural frequencies and modes of vibrating systems. Int. J. Mech. Sci. **1**, 350–355 (1980)

9. Wong, C.N., Zhu, W.D., Xu, G.Y.: On an iterative general-order perturbation method for multiple structural damage detection. J. Sound Vib. **273**(1–2), 363–386 (2004)
10. Wong, C.N., Chen, J.C., To, W.M.: Eigenparameter perturbation method for structural damage detection. 37th AIAA/ASME/ASCE/AHSASC Structural Forum, Salt Lake City UT, 76-ASF-9:658–667 (1996)
11. Wong, C.N., Chen, J.C., To, W.M.: Model updating of a suspension bridge model using parametric perturbation method. Proceedings of Asia-Pacific Vibration Conference '95, Kuala Lumpur, Malaysia. **2**:241–246 (1995)
12. Chen, S.H.: Matrix perturbation method of degenerate vibration systems. J. Jilin Univ. Technol. **4**, 11–15 (1981)
13. Hu, H.C.: Natural vibration theory of multi-degree-of-freedom structures. pp. 17–24. China Science Press, Beijing (1987)
14. Chen, S.H., Liu, Z.S., Shao, C.S., Zhao, Y.Q.: Perturbation analysis of vibration modes with close frequencies. Commun. Num. Methods Eng. **9**, 427–438 (1993)
15. Wanxie, Z., Gengdong, C.: Second-order sensitivity analysis of multimodal eigenvalues and related optimization techniques. Mech. Based Des. Struct. Mach. **14**(4), 421–436 (1986)
16. Wicher, J., Nalecz, A.G.: Second order sensitivity analysis of lumped mechanical systems in the frequency domain. Int. J. Num. Methods Eng. **24**, 2357–2366 (1987)
17. Ryland, G. II., Meirovitch, L.: Response of vibrating systems with perturbed parameters. J. Guid. Control **3**(4), 125–131 (1980)
18. Kan, C.L., Chopra, A.K.: Elastic earthquake analysis of torsionally coupled multistorey buildings. Earthq. Eng. Struct. Dyn. **5**(4), 395–412 (1977)
19. Hejal, R., Chopra, A.K.: Elastic earthquake analysis of a class of torsionally coupled buildings. Earthq. Eng. Struct. Dyn. **18**(3), 305–323 (1989)
20. Tsicnias, T.G., Hutchinson, G.L.: A note on the perturbation analysis of the mode shapes of torsionally coupled buildings. Earthq. Eng. Struct. Dyn. **10**(1), 171–174 (1982)
21. Zhu, W.D., Wong, C.N., Xu, G.Y.: Iterative method to detect structural damage using vibration characteristics. Baltimore Gas and Electric Corporation. Technical report 10-2003 (2003)
22. Patalambros, P.Y., Wilde, D.J.: Principles of optimal design—modeling and computation. pp. 338–343. 2nd edn. Cambridge University Press, New York (2000)